JOC The Journal of Organic Chemistry

Article

Preparation and Physicochemical Properties of [6]Helicenes Fluorinated at Terminal Rings

Vladimir Cirkva, Pavel Jakubík, Tomáš Strašák, Jan Hrbac, Jan Sykora, Ivana Cisarova, Jan Vacek, Jaroslav Žádný, and Jan Storch

J. Org. Chem., **Just Accepted Manuscript** • DOI: 10.1021/acs.joc.8b02870 • Publication Date (Web): 25 Jan 2019

Just Accepted

ACS Publications

is published by the American Chemical Society. 1155 Sixteenth Street N.W., Washington, DC 20036

Preparation and Physicochemical Properties of [6]Helicenes Fluorinated at Terminal Rings

Vladimír Církva,[†*[a‡]] Pavel Jakubík,[†[a‡]] Tomáš Strašák,[[a§]] Jan Hrbáč,[[b]] Jan Sýkora,[*[a⊥]] Ivana Císařová,[[c]] Jan Vacek,[*[d]] Jaroslav Žádný,[[a‡]] and Jan Storch[[a‡]]

[a‡] *Department of Advanced Materials and Organic Synthesis, Institute of Chemical Process Fundamentals of the Czech Academy of Sciences, v. v. i., Rozvojová 135, 165 02 Prague 6, Czech Republic*

[a§] *Department of Bioorganic Compounds and Nanocomposites, Institute of Chemical Process Fundamentals of the Czech Academy of Sciences, v. v. i., Rozvojová 135, 165 02 Prague 6, Czech Republic*

[a⊥] *Department of Analytical Chemistry, Institute of Chemical Process Fundamentals of the Czech Academy of Sciences, v. v. i., Rozvojová 135, 165 02 Prague 6, Czech Republic*

[b] *Institute of Chemistry, Masaryk University, Kamenice 5, 625 00 Brno, Czech Republic*

[c] *Department of Inorganic Chemistry, Faculty of Science, Charles University in Prague, Hlavova 2030, 128 40 Prague 2, Czech Republic*

[d] *Department of Medical Chemistry and Biochemistry, Faculty of Medicine and Dentistry, Palacký University, Hněvotínská 3, 775 15 Olomouc, Czech Republic*

[†]*These authors contributed equally to the paper as first authors.*

E-mails: cirkva@icpf.cas.cz, sykora@icpf.cas.cz, jan.vacek@upol.cz

GRAPHICAL ABSTRACT

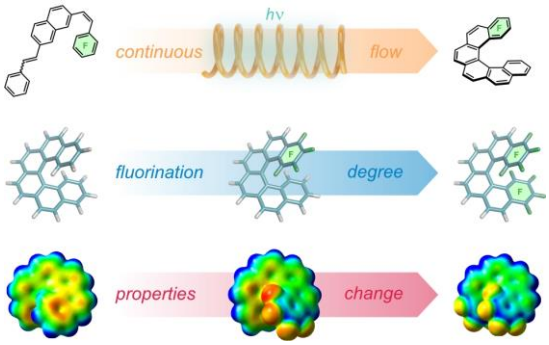

ABSTRACT

The first racemization-stable helicene derivatives fluorinated at terminal rings, 1,2,3,4-tetrafluoro[6]helicene (**6**) and 1,2,3,4,13,14,15,16-octafluoro[6]helicene (**15**), were synthesized via the Wittig reaction followed by oxidative photocyclization in an overall yield of 41% of **6** and 76% of **15**. The changed electronic structure in fluorinated helicenes was reflected in a slight shift of UV-Vis absorption, fluorescence excitation and emission spectra maxima when compared to unsubstituted [6]helicene. Cyclic voltammetry revealed a moderate decrease in the HOMO-LUMO gap with increasing fluorination. The

specific rotation of tetrafluoro[6]helicene **6** enantiomers was found to be approximately 25% lower than that of unsubstituted [6]helicene. The theoretical study of the racemization barrier suggested reasonable shift towards higher energy with increasing fluorination. The increasing fluorination also significantly affected the intermolecular interactions in the crystal lattice. The observed CH···F interactions led to the formation of 1D-molecular chains in the crystal structures of both fluorinated helicenes.

INTRODUCTION

Helicenes are polyaromatic hydrocarbons (PAHs) with nonplanar screw-shaped helical π-skeletons formed by *ortho*-fused benzene rings, where the helical structure is a consequence of the steric repulsion of the terminal aromatic nuclei. Compared to other planar π-conjugated systems, helicenes are chemically stable and more soluble in common organic solvents. Moreover, helicenes are inherently chiral and can be easily resolved into individual enantiomers. The racemization of the first stable representative, hexahelicene, takes place at a significantly elevated temperature. The highly delocalized π-electron system with inherent chirality concentrates unique optical and electronic properties in a single molecule which has attracted scientific interest for decades.[1-11] The exceptionally high values of specific rotation and strong circular dichroism have led to promising applications in materials science, nanoscience, asymmetric catalysis, biological chemistry, supramolecular and polymer chemistry.[3,11]

The very first synthesis of [6]helicene was accomplished via a twelve-step route in 1956.[12] Since then, a number of methods for helicene synthesis have been introduced.[12–19] Among other approaches, the photochemical method (i.e. oxidative photocyclization) seems to be the most flexible and therefore the most used in helicene chemistry up to now.[2,8,20–34] The original synthesis established by Mallory[31] is based on the UV-light induced *cis*/*trans* photoisomerization of stilbene derivative followed by a symmetry-allowed conrotatory electrocyclization of the *cis* isomer to generate *trans*-dihydrophenanthrene derivative as an intermediate. In the presence of air and a catalytic amount of iodine, the intermediate is immediately converted by dehydrogenation into a fully aromatic compound. Over time, this method has been adapted to the synthesis of various substituted helicenes via their stilbene precursors. The improved photochemical methods employed propylene oxide[33], cyclohexene[34] or THF[20], for example, to act as scavengers of forming hydroiodic acid. Recently, the air-driven potassium iodide-mediated oxidative photocyclization of stilbenes has been reported[26] and electrodeless discharge lamps as a novel light source in a microwave reactor have been introduced.[22,23]

The elimination method of hydrogen fluoride called photocyclodehydrofluorination for the synthesis of partially fluorinated PAHs from corresponding fluorinated stilbenes has recently been described.[25] The introduction of fluorine substituents into helicene skeletons is a prospective strategy for tuning the properties required for application in organic electronic devices. Fluorine substitution can affect C-H/π interactions, which prevail in a molecular assembly in the solid state, or can improve the solubility. This

substitution also modulates the HOMO-LUMO gap.[35,36] Generally, fluorine substitution can induce changes in crystal structures, properties of compounds, and also in chemical reactivity. The chemistry of fluorinated PAHs has been the subject of several reviews and monographs.[37–47] The examples of partially fluorinated polyaromatics with *ortho*-fused rings are shown in Figure 1. Tetrafluorophenanthrene (**I**), tetrafluorotriphenylene (**II**), tetrafluorobenzo[*c*]phenanthrene (**III**), and octafluoronaphtho[1,2-*g*]chrysene (**V**) have been prepared by the above-mentioned photocyclodehydrofluorination reaction.[25] These compounds can be prepared also by other methods, for example **I**[44–46], **II**[47,48], and **III**[49]. On the other hand, tetrafluoronaphtho[1,2-*g*]chrysene (**IV**) was prepared on purpose as a blue luminescent[47] and used both in solution and the solid state.

Figure 1. Partially fluorinated polyaromatics.

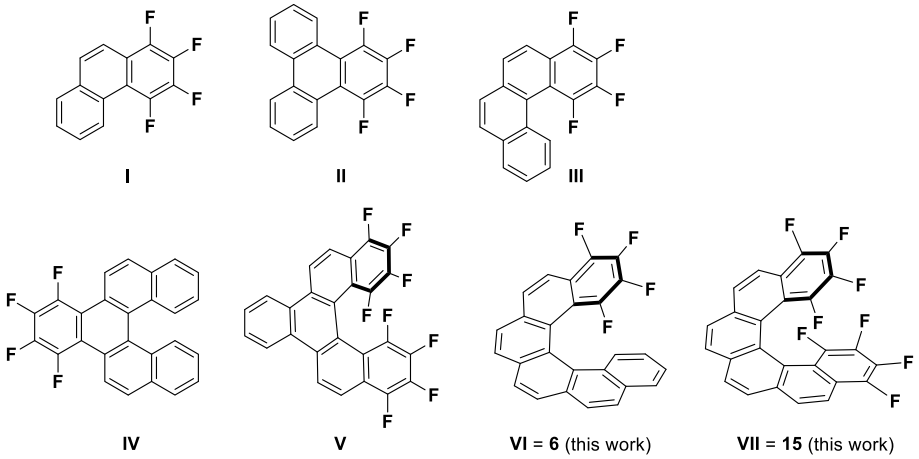

Here we present the first synthesis of partially fluorinated [6]helicenes (**VI** and **VII**) accompanied by optical and electrochemical characterization supported by DFT calculations in order to understand the impact of fluorine substitution on the properties of the synthesized compounds.

RESULTS AND DISCUSSION

Synthesis

Two routes for synthesis of tetrafluoro[6]helicene **6** were developed. Route A uses photocyclodehydrofluorination of the pentafluorinated precursor **3** (Scheme 1) while route B employs oxidative photocyclization of tetrafluorinated precursors **10** and **12** (Scheme 2). The more effective route B was also exploited in the final synthesis of octafluoro[6]helicene **15** by photocyclization of the octafluorinated bis-stilbene precursor **14**.

The palladium(II)-catalyzed Mizoroki-Heck cross-coupling reaction or its sequence was used in order to prepare fluorinated bis-stilbene precursors **3** and **4** (Scheme 1). The reaction of 2,7-naphthalene bistriflate (**1**) and styrene in DMA at 150 °C provided the desired mono-stilbene precursor **2** in 40 % yield. The

subsequent reaction of **2** and pentafluorostyrene provided bis-stilbene **3** in 55 % yield. This reaction was performed in a microwave reactor reducing reaction time significantly. Likewise, the microwave-promoted Mizoroki-Heck reaction of 2,7-naphthalene bistriflate (**1**) and pentafluorostyrene provided fluorinated helicene precursor **4** in 62 % yield. In both cases, (*E*,*E*)-isomers **3** and **4** were obtained as major products according to ^{1}H NMR analysis (see Experimental Section and Supporting Information). Fluorinated 2,7-distyryl-naphthalene **3** was then irradiated through a Pyrex glass jacket in toluene for 3 h in the presence of iodine. Unfortunately, this reaction provided mainly tetraarylcyclobutane derivative **7** as a major product (79 % yield). The formation of **7** is a result of consecutive reaction of the partially cyclized stilbene **5** with (*E*) configuration. Beside the heteronuclear NMR spectroscopy, the structure of **7** was confirmed by X-ray crystallography revealing the *trans* arrangement of the benzo[*c*]phenanthrenyl groups (see Supporting Information). Formation of this photodimer was observed on similar substrates and the resulting geometry is referred to as the centrosymmetric *HT* (*Head-to-Tail*) *anti* stereoisomer.[50] Nevertheless, the reaction also provides the desired fluorinated [6]helicene **6** in a negligible overall yield (2%) as confirmed by NMR spectroscopy and X-ray crystallography (*vide infra*). The whole photocyclodehydrofluorination reaction providing compound **6** proceeded via isomerization of *trans*-**5** to *cis*-**5** followed by the photocyclization and HF elimination from *trans*-pentafluoro-dihydro[6]helicene (Scheme 1).

Scheme 1. Synthetic route A

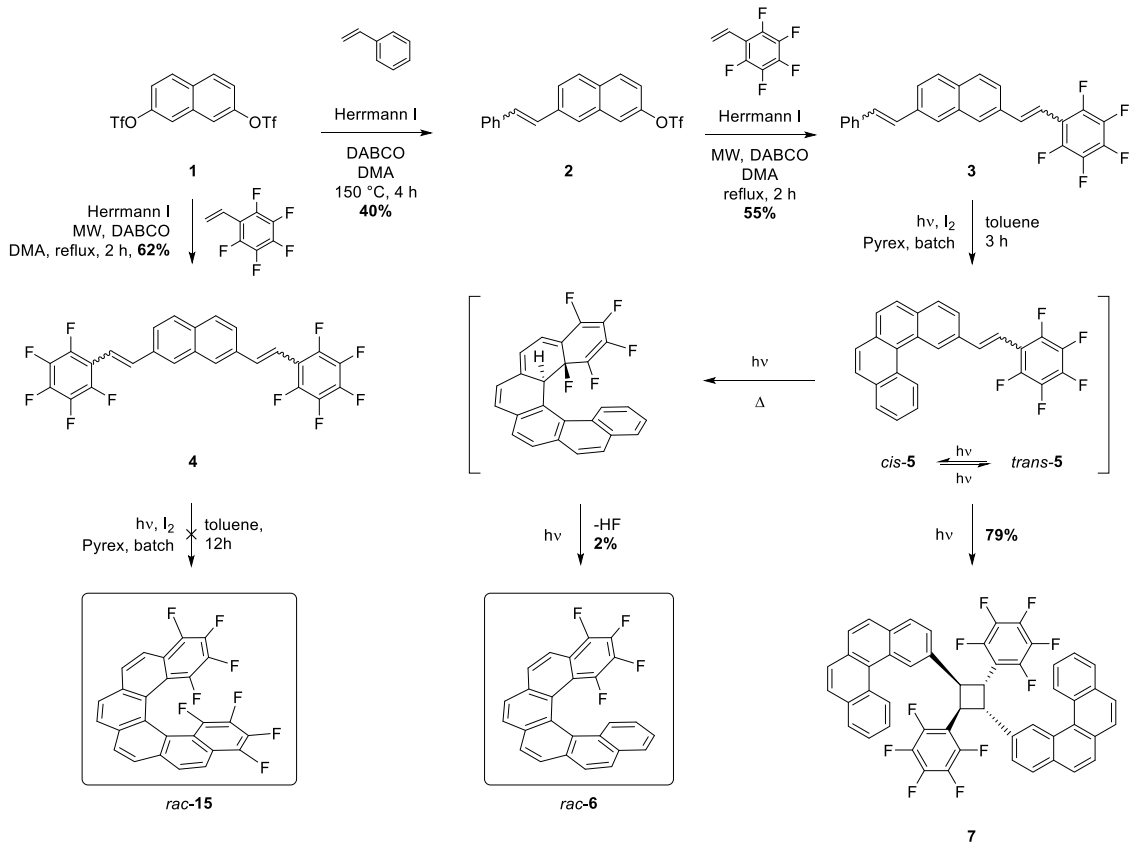

Attempts to prepare octafluoro[6]helicene **15** (Scheme 1) by route A failed. The fluorinated helicene precursor **4** was irradiated through Pyrex glass jacket in the presence of iodine in toluene but, no

photocyclization reaction to **15** was observed even after prolonged reaction time (12 h). The photodimerization reaction did not take place as well, the starting compound **4** was recovered only.

The photocyclodehydrofluorination reaction[25] is not sufficiently effective in the case of fluorinated helicene formation. However, the synthesis of desired fluorinated helicenes can still be furnished via classic Mallory photocyclization.[31] For this purpose, a suitable 2,3,4,5-tetrafluoro derivatives **10**, **12** and **14** were synthesized. Route B (Scheme 2) began with the synthesis of (2,3,4,5-tetrafluorobenzyl)triphenylphosphonium bromide (**9**) that can be reacted with benzo[*c*]phenanthrene-2-carbaldehyde[19] (**8**) or (*E*)-4-[2-(2-naphthalenyl)ethenyl]benzaldehyde[51] (**11**) to corresponding tetrafluorinated stilbenes **10** or **12** in 71 % and 74 % yield, respectively. The reaction provided (*E*)-**10** isomer and a mixture of (*E*,*E*)- and (*E*,*Z*)-**12** isomers. The reaction products were analyzed by LC-NMR (see Experimental Section and Supporting Information) with no isolation of individual isomers, since the subsequent irradiation gives rise to a rapid interconversion of (*E*)- into (*Z*)-isomer.

Scheme 2. Synthetic route B

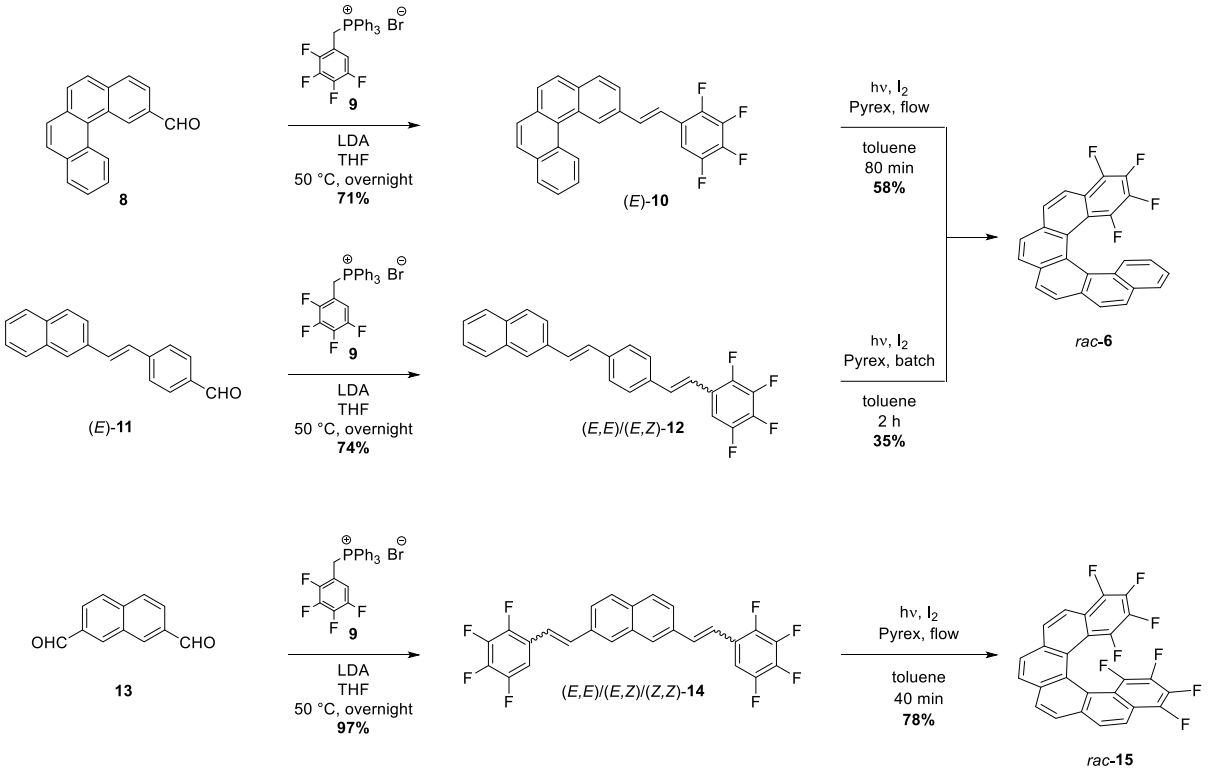

The obtained precursor **10** was dissolved in toluene and irradiated through a Pyrex glass jacket (in a continuous-flow setup) in the presence of iodine for 80 min. Photocyclization provided the desired 1,2,3,4-tetrafluoro[6]helicene (**6**)[52] in 58 % yield. No other regioisomer was identified in the reaction mixture indicating that the ring-closure of stilbene **10** takes place at the *peri* position of the tetracyclic moiety.[53] The mixture of (*E*,*E*)- and (*E*,*Z*)-isomers of the precursor **12** was directly subjected to irradiation. The double photocyclization of precursor **12** (in batch setup) led to helicene **6** in 35 % yield. The synthesis of octafluoro[6]helicene **15** was attempted using 2,7-naphthalenedicarbaldehyde (**13**) which was transformed

via the Wittig reaction with phosphonium salt **9** to the corresponding octafluorinated bis-stilbene precursor **14** in 97 % yield. The reaction products were analyzed by LC-NMR and all three (*E*,*E*), (*E*,*Z*), and (*Z*,*Z*)-**14** isomers were identified. The precursor **14** was then irradiated for 40 min through a Pyrex glass jacket (in a continuous-flow setup) in the presence of iodine in toluene. The photocyclization provided the desired 1,2,3,4,13,14,15,16-octafluoro[6]helicene (**15**) in 78 % yield (the overall yield 76%) as yellow crystals. No other regioisomers were isolated from the reaction mixture. The structure was characterized namely by ^{1}H and ^{19}F NMR due to its low solubility (ca 0.5 mg/mL in chloroform). However, the obtained crystals were submitted to a single crystal X-ray crystallography, which finally confirmed the compound identity (*vide infra*).

UV-Vis Absorption and Fluorescence Spectroscopy

In order to evaluate the effect of fluorine atoms on helicene optical properties the basic spectroscopic methods were applied. The UV-Vis absorption and fluorescence excitation spectra of the fluorinated helicenes **6** and **15** do not differ fundamentally from the spectra of [6]helicene[54–56] (Figure 2). A wavelength close to the excitation maximum (325 nm) was subsequently used for fluorescence emission spectra measurement. The fluorescence originates from the $^{1}L_b$ state, which is not observed in the absorption spectra. The band contains two maxima coming from the S_0 symmetrical vibrational mode and a weaker unresolved shoulder at lower energies (Figure 2C). The high energy edges are equal for fluorinated helicenes **6** and **15**, and exhibit 15 nm bathochromic shift with respect to the fluorescence of unsubstituted [6]helicene. The intensity of the 0-1 transition significantly decreases with increasing degree of fluorination, indicating that the Frank-Condon displacement of nuclear configurations in S_0 and S_1 states is lower than in the original [6]helicene.[54] The fluorescence quantum yields in benzene were determined to be 2.6 % for [6]helicene, 3.3 % for tetrafluoro[6]helicene **6** and 4.6 % for octafluoro[6]helicene **15**.

Figure 2. Normalized absorption (A), fluorescence excitation (B) and emission (C) spectra of [6]helicene (in grey) and its fluorinated derivatives **6** (in blue) and **15** (in red) in benzene.

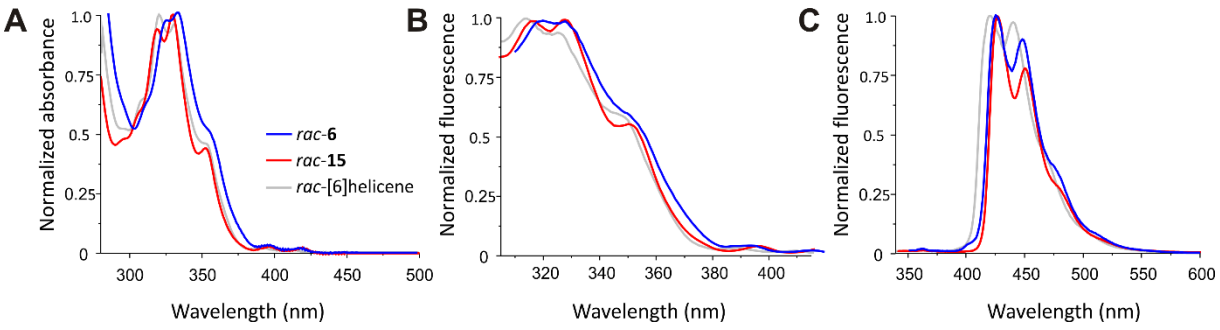

Cyclic Voltammetry

Redox properties of the studied fluorinated [6]helicenes **6** and **15** were investigated by cyclic voltammetry at a glassy carbon electrode using acetonitrile supported by tetrabutylammonium perchlorate (TBAP) as an electrolyte. The concentration of helicenes was chosen to be 10^{-4} M, at the upper solubility limit of **15**.

Cyclic voltammograms of fluorinated [6]helicenes **6** and **15** are shown in Figure 3 along with the voltammogram of unsubstituted [6]helicene[57].

Figure 3. Full (A) and anodic (B) cyclic voltammograms of 0.1 mM [6]helicene and its fluorinated derivatives **6** (in blue) and **15** (in red) in ACN/0.1 M TBAP supporting electrolyte at a glassy carbon electrode (scan rate: 100 mV/s).

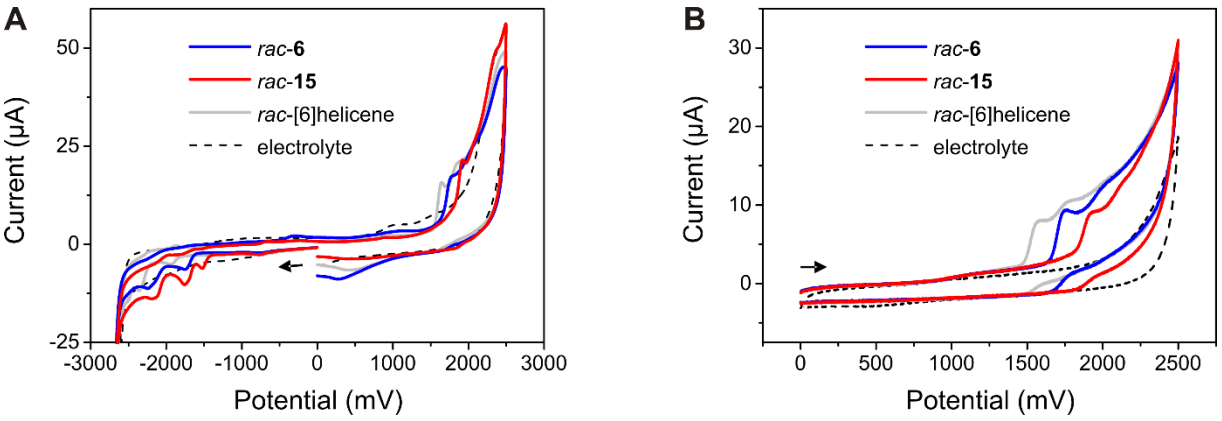

A cathodic scan (Figure 3A) revealed a multistep reduction process, manifested as three rather broad reduction CV peaks. The CV pattern is shifted towards positive potentials with increasing degree of fluorination, indicating that the reduction is facilitated after the functionalization. On the other hand, in anodic CV scans, performed either after cathodic scan or directly (Figure 3B), two overlapped peaks merging with the anodic limit occurred. The anodic features are shifted towards positive potentials with increasing fluorination. The quantification of onset potentials of the first cathodic and of the first anodic CV peaks is a well-established method providing the estimation of the energy levels in organic molecules.[58–60] The onset potentials, determined by the graphical method[60] were converted to an absolute scale and expressed in eV to give an estimation of the HOMO and LUMO energies. While both HOMO and LUMO levels decrease with the degree of fluorination, the overall changes in the HOMO-LUMO gap are negligible (Figure 4B, *vide infra*).

DFT Study

The effect of fluorine substitution is well illustrated also in the comparison of electrostatic potentials mapped onto the electron density surface (Figure 4A) calculated for fluorinated helicenes **6**, **15** and parent [6]helicene. As expected, the strongly electronegative regions were found in the proximity of fluorine atoms. Fluorine substituents of tetrafluoro[6]helicene **6** are more negatively charged than analogous parts of octafluoro[6]helicene **15**, due to the mutual competition of two fluorinated rings in sharing electron density through an aromatic system.

The calculated HOMO and LUMO representations of the studied compounds are presented in Figure 4B, showing the electron density distribution is pronounced in the non-fluorinated rings in each case. The obtained trend in calculated values follows the trend obtained experimentally from CV measurement. While

the HOMO-LUMO gap is almost independent of the substitution, the HOMO and LUMO energy levels decrease within the degree of fluorination (Figure 4B). It is well known that DFT tends to underestimate the intramolecular stabilization in helical structures.[61] This phenomenon is especially reflected in differences between the experimental and calculated LUMO energies. Nevertheless, for a relative evaluation of similar systems this method is abundantly used in the recent literature in a similar manner.[62,63] For more details on DFT calculation see Supporting Information.

Figure 4. (A) Electrostatic potentials calculated for [6]helicene and partially fluorinated derivatives **6** and **15** in the range from -0.04 (red) to 0.04 (blue); (B) Computational (DFT method [B3PW91/6-311++G(d,p)] (in black)) and experimental (CV measurements (in grey)) values of HOMO/LUMO/gap energies for [6]helicene and partially fluorinated derivatives **6** and **15**.

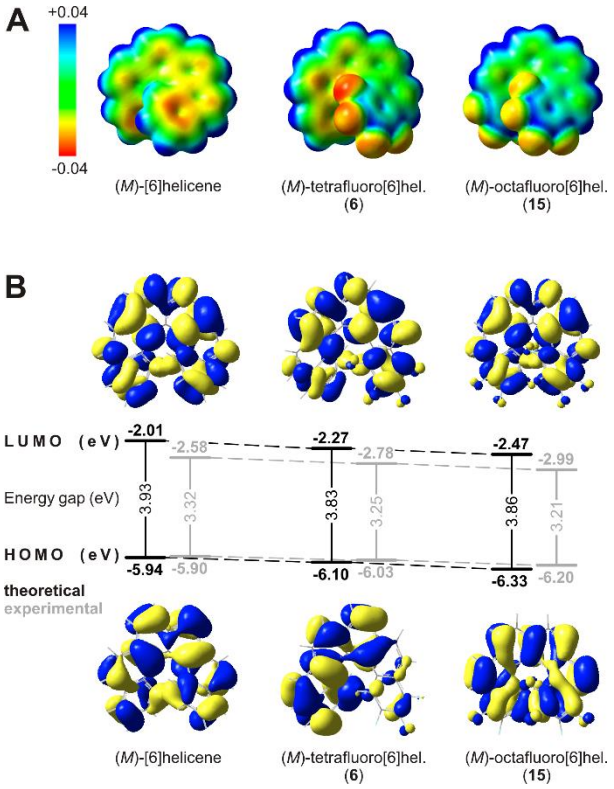

Separation of Enantiomers, CD Spectra, Optical Rotation and Racemization Barrier

Helicenes are valued especially for their chiroptical properties. Therefore, attempts to resolved the fluorinated helicenes **6** and **15** were made. The enantiomeric resolution of tetrafluorinated helicene **6** was accomplished by HPLC using a preparative Kromasil Cellucoat column and *n*-heptane/2-propanol as a mobile phase (for details see Supporting Information).[64] The preparative HPLC was not attempted in the case of octafluorinated helicene **15** due to its low solubility (e.g., only 0.5 mg/mL in chloroform).

The enantiomers of tetrafluoro[6]helicene **6** showed high specific optical rotation. According to the X-ray structure analysis, the dextrorotatory enantiomer was attributed to the *P* form and levorotatory to the *M* form. The obtained specific rotation values (+)-(*P*)-**6** $[\alpha]_D^{20}$ = +2882 ± 4° ($CHCl_3$, *c* 0.0257, >99.5% *ee*)

and for (-)-(*M*)-**6** $[\alpha]_D^{20}$ = -2849 ± 4° ($CHCl_3$, *c* 0.0265, >99.5% *ee*) were lower than values published for unsubstituted [6]helicene ($[\alpha]_D^{24}$ = +3707° and -3640°).[12] This observation can be attributed to a lower electron density and also a shorter distance between terminal rings found for **6** in comparison with [6]helicene in solution[52].

Tetrafluoro[6]helicene **6** enantiomers exhibited clear mirror images in the CD spectra (see Figure 5). Both enantiomers displayed a CD spectrum similar to that of [6]helicene. In the case of the (*P*)-enantiomer, two strong negative bands at 246 and 265 nm (Δε = -306 and -143 M^{-1} cm^{-1}, respectively) along with positive bands at 294, 315, 330 and 353 nm (Δε = +104, +158, +452 and +190 M^{-1} cm^{-1}) were found. A broad peak with a maximum at λ ≈ 330 nm exhibits a slight redshift (in comparison with [6]helicene) and properly correlates with the absorption maximum found at approx. 330 nm (see Figure 2A, *vide supra*).

Figure 5. CD spectra (*c* 10^{-4} M, $CHCl_3$, 25 °C) of (+)-(*P*)-**6** (solid blue) and (-)-(*M*)-**6** (dashed blue) and (+)-(*P*)-[6]helicene[64] (grey, 0.154 mM in THF).

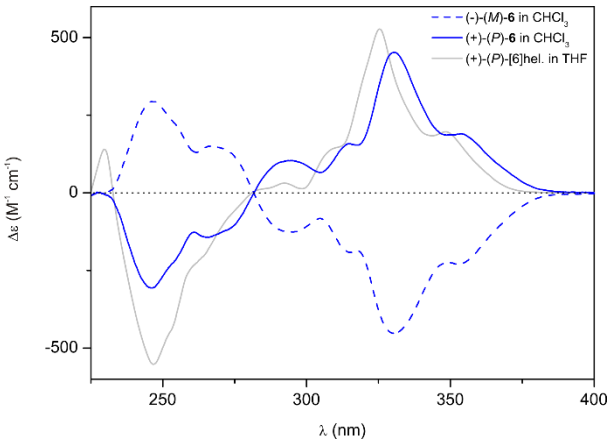

It is well documented that helicenes racemize.[5,65–70] In the case of [6]helicene, the conformational interconversion takes place at elevated temperature and is characterized by the Gibbs free energy barrier $\Delta G^{\ddagger}$ (503 K) = 36.5 kcal mol^{-1} (152.8 kJ mol^{-1}) at 230 °C.[69] On the other hand, the racemization barrier of 1,2,3,4-tetrafluoro[6]helicene (**6**) can be significantly affected by the introduction of bulkier fluorine substituents into the interior of the helix.[8] Therefore, it can be reasonably expected that enantiomers of **6** should possess a higher racemization barrier and provide better thermal stability than unsubstituted [6]helicene. The thermal racemization process was monitored at 233 °C following the decay of the *ee* over time (*t*). The plot of $\ln(ee_t/ee_0)$ against *t* allowed the determination of $\Delta G^{\ddagger}$ (506 K) = 38.9 kcal mol^{-1} (162.9 kJ mol^{-1}) (for details see Supporting Information). Indeed, the obtained value is higher than that reported for unsubstituted [6]helicene (37.2 kcal mol^{-1} extrapolated for 506 K) and smaller than that found for 1-methyl[6]helicene (43.5 kcal mol^{-1} extrapolated for 506 K)[69] where the methyl group effectively hinders the racemization. The DFT calculation of the transition states of the racemization confirmed the assumption that the increasing fluorine substitution increases the racemization barrier and provided corresponding feedback to the experimental data. The $\Delta G^{\ddagger}$ calculated at 298 K for unsubstituted [6]helicene,

tetrafluro[6]helicene **6** and octafluro[6]helicene **15** is 37.3, 38.4 and 41.7 kcal mol^{-1}, respectively (for calculation details see Supporting Information). According to the calculation, the racemization of unsubstituted [6]helicene and octafluro[6]helicene **15** proceeds via a C_s symmetrical transition state while the transition state of tetrafluro[6]helicene **6** is significantly distorted (Figure 6).

Figure 6. (A) Calculated transition states of [6]helicene, tetrafluro[6]helicene **6** and octafluro[6]helicene **15**; (B) Energy diagram of transition states and the overlay of the involved molecules.

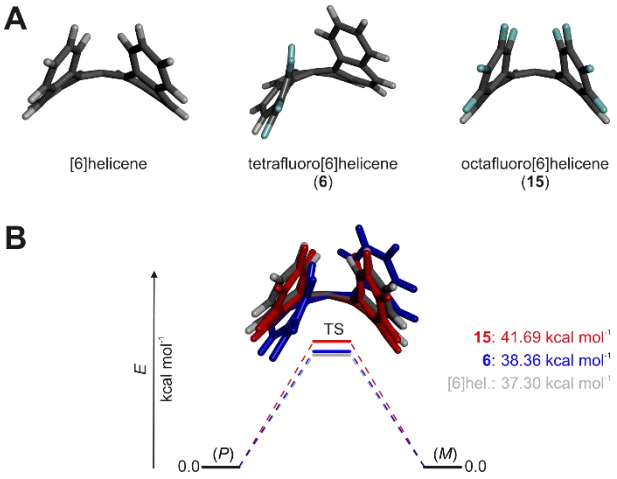

X-ray Crystallography

Recently, the centrosymmetric structure of 1,2,3,4-tetrafluoro[6]helicene (**6**) with *P2₁/n* symmetry was reported in the study dedicated to the dynamic behavior of [6]helicenes.[52] In a racemic form, this compound shows polymorphism and crystallizes also in non-centrosymmetric space group *P2₁2₁2₁*, most likely undergoing lamellar twinning similar to racemic unsubstituted [6]helicene.[71] Furthermore, the single crystals of pure enantiomers of **6** were obtained and analyzed by X-ray crystallography. Both structures of pure enantiomers were identical with the non-centrosymmetric structure of 1,2,3,4-tetrafluoro[6]helicene (**6**). Despite the disorder found in both structures, the refinement of the Flack parameter confirmed the *P* enantiomer as dextrorotational and *M* as levorotational, which is in agreement with the original proposal for [6]helicene derivatives.[72]

All the structures of partially fluorinated [6]helicenes presented in this study utilize a similar motif in the crystal packing, a pair of two mutually interlocked helicene molecules. This motif is well known from the structures of unsubstituted helicenes; however no isostructurality was found. The distance between the helicene peripheral rings found in the presented structures fall into the interval determined for unsubstituted [6]helicene[52], where the distance between C2 and C15 atoms can range from 3.9 to 4.6 Å (Figure 7A). The analysis of accessible crystal structures of basic [6]helicene derivatives ([6]helicene[52], 2-chloro[6]helicene[73] and 2-bromo[6]helicene[72]) shows a significant dependence of the helicene pitch opening on the intermolecular distance between two interlocking molecules, rather than on the helicene substitution (Figure 7B). The helicene pitch enlarges with the shortening of the intermolecular distance

between two interlocking molecules. Generally, the "intercalation" of another molecule into the helicene pitch causes the stretching of the helicene molecule.

Figure 7. (A) Crystal structures of [6]helicene[52], tetrafluro[6]helicene **6** and octafluro[6]helicene **15**; (B) Dependence of the helicene pitch opening on the intermolecular distance between two interlocking molecules of helicenes.

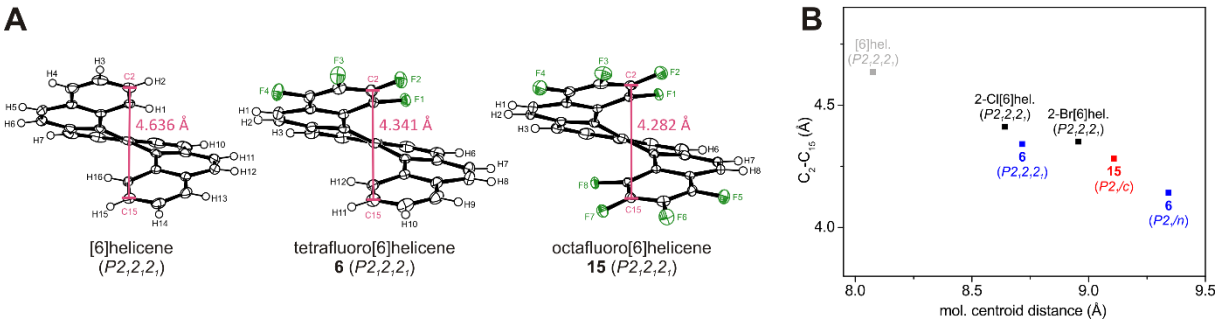

The presence of fluorine atoms in a [6]helicene molecule affects the molecular packing significantly. While molecules of unsubstituted [6]helicene are tied together in the crystal packing by a sophisticated network of π···π and CH···π interactions, the presence of fluorine atoms opens new possibilities for intermolecular interactions. The CH···π interactions are partially substituted by CH···F interactions in the non-centrosymmetric structure of 1,2,3,4-tetrafluoro-[6]helicene (**6**) (Figure 8) leading to the formation of 1D-chains along the [100] direction (Figure 8A) and involving the interaction of the peripheral fluorinated ring with the hydrogen H5 (*d*(H-F) = 2.379 Å) or the interaction with H9 (*d*(H-F) = 2.476 Å) along the [001] direction (Figure 8B). The melting point of this crystal modification was found to be between 220-225 °C. Surprisingly, the melting point of the centrosymmetric modification of **6,** which utilizes mainly π···π interactions within molecular packing, was found at a significantly higher temperature between 243-245 °C.

Figure 8. (A, C) 1D-chains via CH···F interactions in the structure of tetrafluoro[6]helicene **6** and octafluoro[6]helicene **15**, respectively; (B, D) Molecular packing of tetrafluoro[6]helicene **6** and octafluoro[6]helicene **15**, respectively and CH···F interactions in both structures.

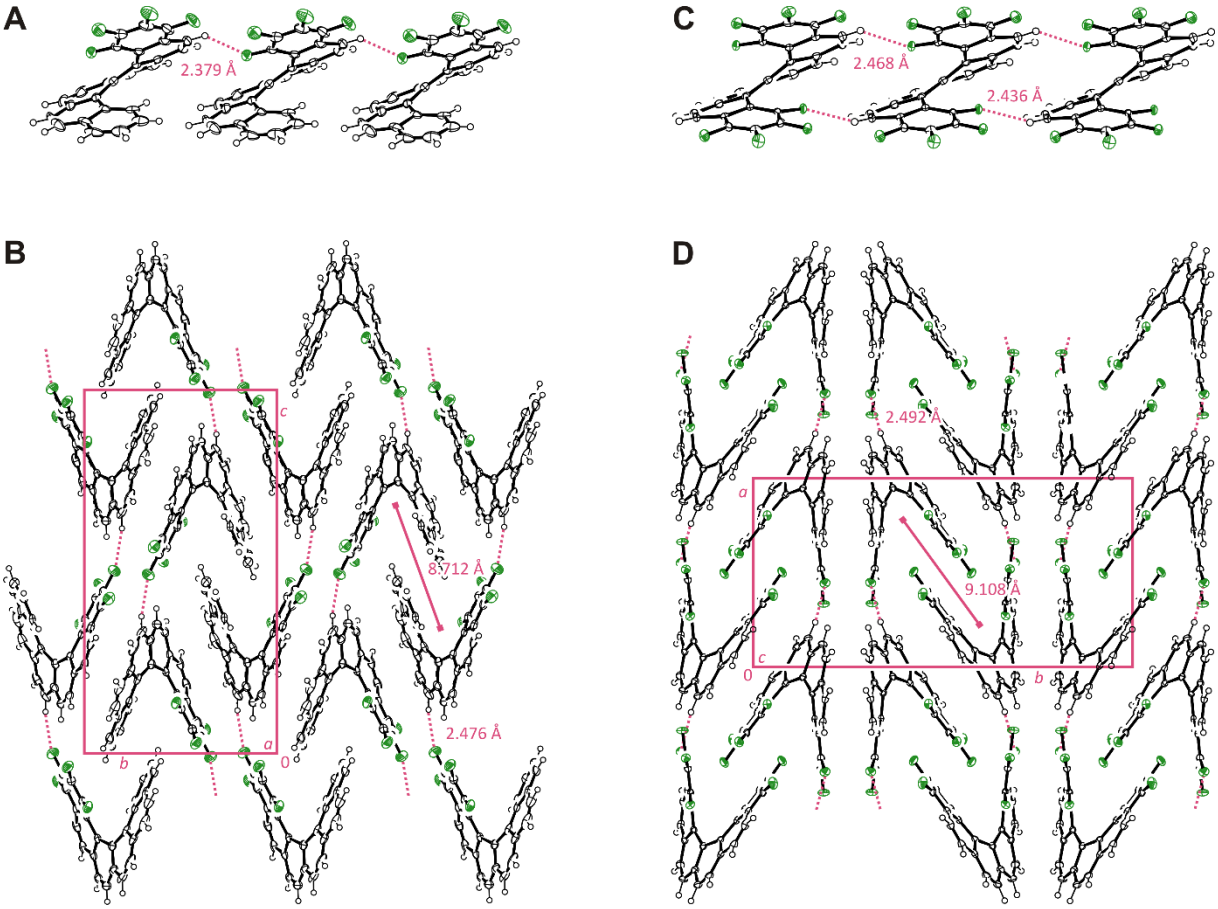

The motif of 1D-chains plays a key role in the molecular packing of octafluoro[6]helicene **15**. The fluorination of both peripheral rings induces the involvement of CH···F interactions on both peripheries of the helicene molecules, leading to a significant strengthening of the mutual interaction between two adjacent molecules in the chain. The H-F distances were found to be 2.436 and 2.468 Å in this structure. These chains can be found along the [001] direction (Figure 8C). Additional intermolecular CH-F interactions can be found along the [100] direction (Figure 8D) between peripheral and central aromatic rings of two proximate molecules (d(H-F) = 2.492 Å). The strengthening of the intermolecular interaction is reflected in a significantly lower solubility and a high melting point. The melting point of octafluoro[6]helicene **15** was not observed below 300°C, despite its sublimation taking place above 330°C.

CONCLUSION

The first racemization-stable helicene derivatives fluorinated at terminal rings, 1,2,3,4-tetrafluoro[6]helicene (**6**) and 1,2,3,4,13,14,15,16-octafluoro[6]helicene (**15**), were successfully synthesized via the Mizoroki-Heck cross-coupling reaction and Wittig reaction, followed by eliminative or

oxidative photocyclization with an overall yield of 41% of **6** and 76% of **15**. It was found that the photocyclodehydrofluorination reaction is not suitable for this purpose (2% yield of **6** and 0% yield of **15**) due to the formation of dimeric structures. The prepared fluorinated helicenes showed similar optical properties when compared to unsubstituted [6]helicene. The changed electronic structure in fluorinated helicenes was reflected in a slight shift of UV-Vis absorption, fluorescence excitation and emission spectra maxima. Cyclic voltammetry revealed a moderate decrease in the HOMO-LUMO gap with increasing fluorination which was found fully in agreement with DFT calculations. The specific rotation of tetrafluoro[6]helicene **6** enantiomers was found to be approximately 25% lower than that of unsubstituted [6]helicene. The characterization of individual octafluoro[6]helicene enantiomers **15** was precluded by low solubility of the compound. The theoretical study of the fluorinated [6]helicenes racemization suggested a reasonable shift towards higher energy barrier with increasing fluorination. The increasing fluorination also significantly affected the intermolecular interactions in the crystal lattice. The π···π and CH···π interactions are gradually substituted by CH···F interactions which constitute 1D-molecular chains in the structures of both fluorinated helicenes. The fluorination of both peripheral rings in **15** enables the formation of very strong intermolecular interactions within the 1D-chain, resulting in an elevated melting point and significantly decreased solubility of the compound **15**. Mainly in this regard, future interest should be focused on tetrafluoro-substituted helicene derivatives.

EXPERIMENTAL SECTION

Commercially available reagent grade materials were used as obtained from Sigma-Aldrich, Acros Organics, Apollo Scientific and Fluorochem excepting 2,3,4,5-tetrafluorobenzoic acid (Fluorochem) that was recrystallized from dichloromethane. Herrmann's catalyst, i.e. *trans*-di(μ-acetato)-bis[*o*-(di-*o*-tolylphosphino)benzyl]dipalladium(II) was prepared according to published procedure[74]. Compound **8** was prepared according to a reaction Scheme S1 (see SI) via synthesis of intermediates (**i**) and (**ii**). Compound **9** was prepared according to a reaction Scheme S2 (see SI) via synthesis of intermediates (**iii**) and (**iv**). All solvents (Lach-Ner) were of a reagent grade and used without any further purification, except for tetrahydrofurane, which was distilled from sodium benzophenone ketyl. Melting points were determined with Santiago KB T300 melting point apparatus (Czech Republic) and are uncorrected. TLC was carried out using Silica gel 60 F_{254}-coated aluminum sheets and compounds were visualized with UV light (254 and 366 nm). Column chromatography was performed using Merck Kieselgel 60 silica gel (230-400 mesh) or Biotage HPFC systems (SP-1 and Isolera One) with pre-packed flash silica gel columns. The standard Schlenk technique was used for all reactions; cannula filtration technique was used for filtrations under inert atmosphere. Microwave experiments were performed on an Anton Paar Monowave 300 equipped with simultaneous temperature measurement with IR sensor. ^{1}H, $^{13}C\{^{1}H\}$, $^{19}F\{^{1}H\}$, and $^{31}P\{^{1}H\}$ NMR spectra were recorded using a Bruker Avance and Varian Inova spectrometer at 400 MHz and 500 MHz, respectively (^{1}H NMR), 101 MHz and 126 MHz, respectively (^{13}C NMR), 376 MHz and 471 MHz,

respectively (^{19}F NMR), and 162 MHz and 202 MHz, respectively (^{31}P NMR). Chemical shifts (δ) are reported in parts per million (ppm) relative to TMS, C_6F_6 (δ = -164.90 ppm) and 85% H_3PO_4 in H_2O, or referenced to residuals of $CDCl_3$ (δ = 7.26 ppm and 77.00 ppm, respectively), $C_2D_2Cl_4$ (δ = 6.0 ppm and 73.78 ppm, respectively), CD_3CN (δ = 1.94 ppm and 118.69 ppm, respectively) and DMSO-d_6 (δ = 2.50 ppm). The coupling constants (*J*) are given in Hertz (Hz) and corresponding multiplicity (s = singlet, d = doublet, t = triplet, m = multiplet). For the LC-NMR experiments, commercial HPLC system (Dionex UltiMate 3000) with 250×4.6 mm HPLC column (Luna C8(2), Phenomenex, 5 μm particles, 100 Å pore size) was employed. 50 μL of the concentrated acetonitrile solution was injected into HPLC. The separation was done by isocratic method by system acetonitrile - D_2O 85:15 % and was monitored at 220 nm and 254 nm and by on-flow ^{1}H NMR detection. ^{1}H NMR observations were conducted on Varian INOVA 500 MHz spectrometer equipped with HCN triple resonance-microflow probe (60 μL active volume). Standard NMR software VnmrJ 4.2 was used. All the separations and NMR detection were conducted at ambient temperature (22 °C). The ^{1}H NMR data were collected in on-flow mode employing WET multiple frequency solvent suppression[75]. The signal of acetonitrile solvent (δ = 2.00 ppm) was suppressed using one scout scan prior to whole data collection. The data acquisition during 1 s acquisition time covering the spectral width of 6 kHz followed after 90° RF pulse (3.4 μs), four transients were accumulated in each spectrum. No relaxation delay was employed. The detailed analysis of chromatographic peaks was performed in the stop-flow mode. ^{1}H NMR spectra were accumulated over 32 scans for cis-cis isomer/256 scans for mixture of cis-cis isomer and cis-trans isomer/512 scans for trans-trans isomer (acquisition time 2 s, relaxation delay 1 s). Absorption spectra were recorded on a Specord 250 spectrometer (Jena Bioscience, Germany) in a quartz cuvette with 1-cm optical path, using a pure solvent as a reference. Steady-state excitation and emission spectra were recorded using F-4500 fluorometer (Hitachi, Japan) in a quartz cuvette with a 1-cm optical path (for both excitation and emission). Electrochemical experiments were conducted using a Nanoampere electrochemical workstation (L-Chem). The IR spectra were measured in $CHCl_3$ (NICOLET 6700). Characteristic IR absorptions are reported in cm^{-1} and denoted as strong (s), medium (m), and weak (w). The low resolution electron impact (EI) mass spectra were recorded on a Thermo Finnigan Focus DSQ mass spectrometer at an ionizing voltage of 70 eV in a positive mode and the *m/z* values are given along with their relative intensities (%). For exact mass measurement, the spectra were internally calibrated using Na-formate or APCI-TOF tuning mix. ESI and APCI high-resolution mass spectra were measured in a positive mode using a micrOTOF QIII mass spectrometer (Bruker) and were determined by software Compass Data Analysis. Diffraction data were collected on a Bruker D8 VENTURE Kappa Duo PHOTON 100 CMOS with the monochromated Mo/Cu-Kα radiation. The structures were solved by direct methods (SHELXT[76]) and refined by full-matrix least-squares on F^2 values (CRYSTALS[77] or SHELXL[78,79]). All heavy atoms were refined anisotropically. Hydrogen atoms were usually localized from the expected geometry and difference electron density maps and were refined isotropically. ORTEP-3[80] was used for structure presentation. Resolution of enantiomers was performed on

preparative HPLC with UV detector at 320 nm (Watrex) using chiral stationary phase Kromasil Cellucoat® (Akzo Nobel) column (250 x 16 mm, 10 μm) and *n*-heptane/2-propanol 99.0:1.0 as a mobile phase at a flow rate of 12 mL/min. The optical purity of each enantiomer and racemization process were studied by integration of UV traces (254 nm) of HPLC chromatograms (see Figure S2) at Varian ProStar 230 SDA + ProStar 330 PDA detector (200-400 nm). The HPLC analyses were performed on Kromasil Cellucoat® (Akzo Nobel) column (250 x 4.6 mm, 10 μm) using *n*-heptane/2-propanol 99.65:0.35 as a mobile phase at a flow rate of 2 mL/min. Specific optical rotations ($[\alpha]_D^{20}$) were measured at 589 nm in chloroform at 20 °C on JASCO P-2000 Polarimeter with a Peltier cell holder and a 1 dm path length cell. The values are given in deg cm^3 g^{-1} dm^{-1} as an average value from 50 measurements. The circular dichroism (CD) spectra were acquired on a J-815 spectrometer (Jasco Analytical Instruments, Inc., Easton, USA) in chloroform (1×10^{-4} M), using a 1-mm quartz sample cell.

2-Trifluoromethylsulfonyloxy-7-(2-phenylethenyl)naphthalene (2). Naphthalene-2,7-diyl bis(trifluoromethanesulfonate)[81] (**1**, 25 g, 58.9 mmol, 1 eq), *trans*-di(μ-acetato)-bis[*o*-(di-*o*-tolylphosphino)benzyl]dipalladium(II) (Herrmann's catalyst, 0.55 g, 0.589 mmol, 0.01 eq), diazabicyclo[2.2.2]octane (DABCO) (13.2 g, 118 mmol, 2 eq) and styrene (7.09 mL, 61.9 mmol, 1.05 eq) were charged into 2000 mL round-bottom flask and dissolved in 1000 mL of dimethylacetamide (DMA). Reaction mixture was heated to 150 °C for 4 hours under condenser. After cooling down, methanol (500 mL) was added and the mixture was allowed to precipitate in the freezer (-18 °C) overnight. Filtration was performed to remove palladium and insoluble side products. Filtrate was dry loaded on silica gel and chromatography using petroleum ether-ethyl acetate (20:1) as a mobile phase was performed. Combined fractions were concentrated *in vacuo* and product **2** was spontaneously crystallized to obtain 8.9 g (40 %) of ocher crystals with a majority of (*E*) isomer. mp = 112.5-115 °C. ^{1}H NMR (400 MHz, $CDCl_3$): (*E*) major δ 7.88-7.82 (m, 3H), 7.79 (d, *J* = 8.8 Hz, 1H), 7.73 (d, *J* = 2.4 Hz, 1H), 7.60-7.57 (m, 2H), 7.42 (t, *J* = 7.3 Hz, 2H), 7.36-7.31 (m, 2H), 7.28 (d, *J* = 16.4 Hz, 1H), 7.24 (d, *J* = 16.4 Hz, 1H). ^{13}C {^{1}H} NMR (101 MHz, $CDCl_3$): (*E*) major δ 147.5, 136.8, 136.6, 133.7, 131.8, 130.5, 130.3, 128.8 (2 x C), 128.2, 128.1, 127.7, 126.7 (2xC), 126.2, 124.9, 119.3, 119.1, 118.8 (q, $J_{C\text{-}F}$ = 320.9 Hz, CF_3). ^{19}F {^{1}H} NMR (376 MHz, $CDCl_3$): (*E*) major δ -75.93 (s, 3F). IR (cm^{-1}): 3085, 3063, 1629, 1597, 1579, 1509, 1497, 1449, 1423, 1299, 1240, 1188, 1150, 1141, 1001, 980, 855, 830, 692, 618, 598, 559, 510, 500 cm^{-1}. EIMS *m/z*: 378 (100%, $M^{+\cdot}$), 217 (77%), 202 (74%). HRMS (APCI/TOF) *m/z* M^+ Calcd for $C_{19}H_{13}F_3O_3S$ 379.0610; Found 379.0609.

2-[2-(Pentafluorophenyl)ethenyl]-7-(2-phenylethenyl)naphthalene (3). 2-Trifluoromethylsulfonyloxy-7-(2-phenylethenyl)naphthalene (**2**), (100 mg, 0.264 mmol, 1 eq), *trans*-di(μ-acetato)-bis[*o*-(di-*o*-tolylphosphino)benzyl]dipalladium(II) (Herrmann's catalyst, 5 mg, 5,29 μmol, 2 mol%), DABCO (59 mg, 0.529 mmol, 2 eq) and 2,3,4,5,6-pentafluorostyrene (0.037 mL, 0.316 mmol, 1.2 eq) were charged into 30 mL round-bottom reaction vessel and dissolved in DMA (10 mL). Reaction was heated up to 160 °C in microwave reactor for 2 hours. After cooling down, methanol (10 ml) was added and reaction mixture was allowed to precipitate in freezer (-18 °C) overnight. Precipitate was filtered out and extracted with hot toluene (30 mL) to remove palladium. Solvent was removed *in vacuo* to provide **3** (61 mg, 55 %) as white powder with a majority of (*E*,*E*) isomer. mp 221.0-229.0 °C. ^{1}H NMR (400 MHz, $CDCl_3$): (*E*,*E*) major δ 7.90 (d, *J* = 9.2 Hz, 1H), 7.86 (d, *J* = 9.2 Hz, 1H), 7.83 (d, *J* = 8.6 Hz, 1H), 7.82 (d, *J* = 8.5 Hz, 1H), 7.76 (d, *J* = 8.6 Hz, 1H), 7.70 (d, *J* = 8.5 Hz, 1H), 7.60 (d, *J* = 16.6 Hz, 1H), 7.58 (d, *J* = 7.5 Hz, 2H), 7.40 (t, *J* = 7.5 Hz, 2H), 7.31-7.26 (m, 3H), 7.11 (d, *J* = 16.6 Hz, 1H). ^{13}C {^{1}H} NMR was not determined due to low solubility. ^{19}F {^{1}H} NMR (376 MHz, $CDCl_3$): (*E*,*E*) major δ -145.81 (dd, *J* = 20.8, 7.9 Hz, 2F), -159.58 (t, *J* = 20.8 Hz, 1F), -166.05 (m, 2F). IR (cm^{-1}): 3086, 3058, 1653, 1632, 1620, 1599, 1576, 1522, 1599, 1576, 1449, 1494, 1427, 1310, 1249, 1188, 1159, 1142, 1130, 1027, 1000, 971, 957, 854, 833, 694, 629, 614, 584, 435. EIMS *m/z*: 422 (100%, $M^{+\cdot}$), 228 (11%). HRMS (APCI/TOF) *m/z*: M^+ Calcd for $C_{26}H_{15}F_5$, 422.1094; Found 422.1077.

2,7-Bis[2-(pentafluorophenyl)ethenyl]naphthalene (4). Naphthalene-2,7-diyl bis(trifluoromethanesulfonate)[81] (**1**, 100 mg, 0.236 mmol, 1 eq), *trans*-di(μ-acetato)-bis[*o*-(di-*o*-tolylphosphino)benzyl]dipalladium (II) (Herrmann's catalyst, 9 mg, 9,43 μmol, 4 mol%), DABCO (106 mg, 0.943 mmol, 4 eq) and 2,3,4,5,6-pentafluorostyrene (0.078 mL, 0.566 mmol, 2.4 eq) were charged into 30 mL round-bottom reaction vessel and dissolved in DMA (10 mL). Reaction mixture was heated up to up to 160 °C in microwave reactor for 2 hours. After cooling down, methanol (10 ml) was added and reaction mixture was allowed to precipitate in freezer (-18 °C) overnight. Precipitate was filtered out and extracted with hot toluene (50 mL) to remove the palladium. Solvent was removed *in vacuo* to provide **4** (75 mg, 62 %) as a white powder with majority of (*E*,*E*)-isomer. mp 197.5-200.0 °C. ^{1}H NMR (400 MHz, $CDCl_3$): (*E*,*E*) major δ 7.90 (s, 2H), 7.85 (d, *J* = 8.6 Hz, 2H), 7.74 (dd, *J* = 8.6, 1.5 Hz, 2H), 7.60 (d, *J* = 16.9 Hz, 2H), 7.12 (d, *J* = 16.9 Hz, 2H). ^{13}C {^{1}H} NMR was not observed due to a low solubility. ^{19}F {^{1}H} NMR (376 MHz, $CDCl_3$): (*E*,*E*) major δ -145.74 (m, 4F), -159.33 (t, *J* = 20.7 Hz, 2F), -165.96 (m, 4F). IR (cm^{-1}): 1651, 1636 (CH=CH), 1617, 1598, 1521, 1497, 1430, 1316, 1250, 1144, 1132, 964, 855. EIMS *m/z*: 512 (100%, $M^{+\cdot}$), 492 (13%), 472 (13%), 318 (10%), 256 (10%), 207 (12%). HRMS (APCI/TOF) *m/z*: M^+ Calcd for $C_{26}H_{10}F_{10}$, 512.0623; Found 512.0618.

2-[2-(Pentafluorophenyl)ethenyl]benzo[*c*]phenanthrene (5). Photoreaction in a batch setup (see SI) was followed with bis-stilbene derivative **3** (0.5 g, 1.18 mmol, 1 eq), iodine (0.2 g, 0.79 mmol, 0.67 eq) and toluene (1000 mL). The mixture was irradiated for 3 hours and then washed trough silica pad with sodium thiosulfate to remove excess of iodine and insoluble reaction byproducts. Solvent was removed under reduced pressure and the residue was purified by flash chromatography (RP silica gel, 9:1 acetonitrile/water) to provide **5** (2.5 mg, 0.5 %) as ocher crystals. mp 232.5-235.0 °C. ^{1}H NMR (400 MHz, $CDCl_3$): (*E*) major δ 9.17 (s, 1H), 9.11 (d, *J* = 8.6 Hz, 1H), 8.07-8.04 (m, 2H), 7.94-7.83 (m, 5H), 7.75 (m, 1H), 7.73 (d, *J* = 16.6 Hz, 1H), 7.69-7.64 (m, 1H), 7.19 (d, *J* = 16.6 Hz, 1H). ^{13}C {^{1}H} NMR was not observed due to a low solubility. ^{19}F {^{1}H} NMR (376 MHz, $CDCl_3$): (*E*) major δ -145.73 (m, 2F), 159.61 (t, *J* = 20.7 Hz, 1F), -166.05 (m, 2F). IR (cm^{-1}): 1651, 1631 (CH=CH), 1603, 1521, 1498, 1420, 1363, 1312, 1254, 1147, 1132, 1106, 1036, 971, 962, 860, 799, 658, 621, 574. EIMS *m/z*: 420 (100%, $M^{+\cdot}$), 400 (13%), 226 (16%). HRMS (APCI/TOF) *m/z*: M^+ Calcd for $C_{26}H_{13}F_5$, 420.0937; Found 420.0942.

1,2,3,4-Tetrafluoro[6]helicene (6). Procedure **A**: Photoreaction in a batch setup (see SI) was followed with bis-stilbene derivative **3** (0.5 g, 1.18 mmol, 1 eq), iodine (0.2 g, 0.79 mmol, 0.67 eq) and toluene (1000 mL). The mixture was irradiated for 3 hours and then washed trough silica pad with sodium thiosulfate to remove excess of iodine and insoluble reaction byproducts. Solvent was removed under reduced pressure and the residue was purified by flash chromatography (RP silica gel, 9:1 acetonitrile/water) to provide **6** (10 mg, 2 %) as yellowish crystals. Procedure **B**: 2-[2-(2,3,4,5-Tetrafluorophenyl)ethenyl]benzo[*c*]phenanthrene (**10**) (2.0 g, 4.97 mmol, 1 eq) and iodine (0.2 g, 0.79 mmol, 0.16 eq) were dissolved in toluene (4 L) and subjected to the photoreaction in a continuous flow setup (see chapter 1.2.2.) with a flow rate of 50 $mL.min^{-1}$. Reaction mixture was washed through an in-line column packed with silica gel (30 g) and sodium thiosulfate (50 g) to remove the excess iodine and insoluble byproducts. Solvent was removed under reduced pressure and a recrystallization from DCM/heptane (1:1) provided **6** (1.15 g, 58%) as yellowish crystals. Procedure **C**: 2-[2-(4-(2-(2,3,4,5-Tetrafluorophenyl)ethenyl)phenyl)ethenyl]naphthalene (**12**) (200 mg, 0.495 mmol, 1 eq) and iodine (20 mg, 0.079 mmol, 0.15 eq) were charged into a tall 800 mL beaker, dissolved in toluene (500 mL) and subjected to the photoreaction in a batch setup (see chapter 1.2.1.) for 2 hours. Reaction mixture was washed trough a pad of sodium thiosulfate (30 g) to remove the excess of iodine (toluene), then concentrated *in vacuo* and washed trough a silica pad (15 g, toluene) and evaporated. Recrystallization from DCM/heptane (1:1) provided **6** (70 mg, 35 %) as yellowish crystals. mp 243.5-246.0 °C (*$P2_1/n$*), 220-225 °C (*$P2_12_12_1$*). ^{1}H NMR (400 MHz, $CDCl_3$): δ 8.17 (d, *J* = 8.1 Hz, 1H), 8.16 (dd, *J* = 8.7, 1.6 Hz, 1H), 8.07-8.01 (m, 4H), 7.96 (s, 2H), 7.89 (dd, *J* = 8.0, 1.4 Hz, 1H), 7.30 (ddd, *J* = 8.0, 6.9, 1.1 Hz, 1H), 7.14 (bd, *J* = 8.5 Hz, 1H), 6.74 (ddd, *J* = 8.5, 6.9, 1.4 Hz, 1H) (in agreement with published data in lit.[52]). ^{13}C {^{1}H} NMR (101 MHz, $CDCl_3$): δ 143.5 (m, J_{C-F} = 255.3 Hz), 142.1 (m, J_{C-F} = 248.32 Hz), 138.5 (m, J_{C-F} = 250.6 Hz), 137.6 (m, J_{C-F} = 252.3 Hz), 132.7, 132.4, 131.7, 130.4, 129.1, 129.0, 128.9, 128.4, 128.19, 128.15, 127.8, 126.3,

126.1, 125.92, 125.88, 125.7, 124.7, 124.6, 124.0, 122.3, 118.0, 117.5 (d, J = 10.9 Hz). ^{19}F {^{1}H} NMR (376 MHz, $CDCl_3$): δ -131.90 (m, 1F), -153.05 (dd, J = 20.2, 13.0 Hz, 1F), -162.28 (dt, J = 20.2, 4.8 Hz, 1F), -163.13 (t, J = 20.2 Hz, 1F). IR (cm^{-1}): 1655, 1531, 1510, 1493, 1306, 1182, 1132, 1073, 1015, 927, 582. EIMS *m/z*: 400 (100%, $M^{+\cdot}$), 380 (26%), 372 (10%), 360 (20%), 354 (15%), 336 (11%). HRMS (APCI/TOF) *m/z*: M^+ Calcd for $C_{26}H_{12}F_4$, 400.0875; Found 400.0869. Specific rotation: (+)-(*P*)-6 $[\alpha]_D^{20}$ +2882 ± 4° ($CHCl_3$, *c* 0.0257); (-)-(*M*)-6 $[\alpha]_D^{20}$ -2849 ± 4° ($CHCl_3$, *c* 0.0265).

(1*R*,2*R*,3*S*,4*S*)-1,3-Bis(pentafluorophenyl)-2,4-bis(2-benzo[*c*]phenanthrenyl)cyclobutane (7). Photoreaction in a batch setup (see SI) was followed with bis-stilbene derivative **3** (0.5 g, 1.18 mmol, 1 eq), iodine (0.2 g, 0.79 mmol, 0.67 eq) and toluene (1000 mL). The mixture was irradiated for 3 hours and then washed trough silica pad with sodium thiosulfate to remove excess of iodine and insoluble reaction byproducts. Solvent was removed under reduced pressure and the residue was purified by flash chromatography (RP silica gel, 9:1 acetonitrile/water) to provide **7** (400 mg, 79 %) as pale brown powder. mp n.d. (> 300 °C). ^{1} H NMR (500 MHz, $CDCl_3$): δ 9.04 (s, 2H), 8.87 (d, J = 8.3 Hz, 2H), 8.05 (dd, J = 6.4, 1.6 Hz, 2H), 7.95 (d, J = 8.3 Hz, 2H), 7.92 (d, J = 8.5 Hz, 2H), 7.86 (d, J = 8.5 Hz, 2H), 7.83 (d, J = 8.5 Hz, 2H), 7.82 (d, J = 8.5 Hz, 2H), 7.71-7.64 (m, 4H), 7.52 (bd, J = 8.3 Hz, 2H), 5.34-5.24 (m, 4H). ^{13}C {^{1}H} NMR (126 MHz, $CDCl_3$): δ 136.9, 133.5, 132.4, 131.3, 130.3, 130.1, 129.0, 128.7, 127.7, 127.3, 127.1, 127.0, 126.8, 126.18, 126.15, 126.1, 124.8, 46.2, 39.6. (Quaternary carbons interacting with fluorine nuclei were not detected). ^{19}F {^{1}H} NMR (471 MHz, $CDCl_3$): δ -144.06 (m, 4F), -155.18 (t, J = 21.7 Hz, 2F), -164.87 (dt, J = 21.7, 7.4 Hz, 4F). IR (cm^{-1}): 2855, 1654, 1599, 1523, 1499, 1421, 1361, 1305, 1257, 1137, 1111, 976, 959, 868, 621, 577. HRMS (APCI/TOF) *m/z*: M^+ Calcd for $C_{52}H_{26}F_{10}$, 840.1875; Found 840.1955.

Benzo[*c*]phenanthrene-2-carbaldehyde (8). 2-Bromobenzo[*c*]phenantrene (**ii**) (6.26 g, 20.4 mmol, 1.0 eq) was dissolved in dry THF (150 mL) under argon atmosphere and cooled down to -78 °C. *n*-Butyllithium solution (2.5M in hexanes, 10.6 mL, 26.5 mmol, 1.3 eq) was added dropwise and the mixture was stirred for few minutes. Afterwards, *N*,*N*-dimethylformamide (4 mL, 51.7 mmol, 2.53 eq) was added and reaction was stirred for an additional hour. Excessive *n*-butyllithium was quenched by addition of methanol (10 mL), reaction mixture was extracted with DCM (3 x 100 mL), and combined organic layers were dried over anhydrous magnesium sulfate and filtered. Solvents were removed under reduced pressure and the residue was recrystallized from DCM/methanol (2:1) mixture to provide **8** (5.07 g, 97%) as a white powder. mp 94-95 °C; (lit.[82] mp 94.5-96 °C). ^{1}H NMR (400 MHz, $CDCl_3$): δ 10.29 (s, 1H), 9.60 (s, 1H), 9.08 (d, J = 8.4 Hz, 1H), 8.16−8.09 (m, 2H), 8.08 (dd, J = 7.9, 1.4 Hz, 1H), 8.02−7.94 (m, 3H), 7.87 (d, J = 8.5 Hz, 1H), 7.78 (ddd, J = 6.9, 6.9, 1.5 Hz, 1H), 7.70 (ddd, J = 6.9, 6.9, 1.2 Hz, 1H) (in agreement with published data in lit.[19]). HRMS (APCI/TOF) *m/z*: $[M+H]^+$ Calcd for $C_{19}H_{13}O$, 257.0961; Found 257.0959.

(2,3,4,5-Tetrafluorobenzyl)triphenylphosphonium bromide (**9**)[49]. Into a solution of 2,3,4,5-tetrafluorobenzylbromide (**iv**) (3.0 g, 13.35 mmol, 1 eq) in toluene (300 mL), triphenylphosphine (3.56 g, 13.58 mmol, 1.1 eq) was added and the mixture was heated up to reflux overnight. The reaction mixture was cooled down to room temperature and the reaction mixture was concentrated to one third of volume under reduced pressure. The precipitate was filtered out and washed with toluene (50 mL) to provide **9** (5.45 g, 87 %) as a white powder in a satisfactory purity. mp 222.5-223.9 °C. ^{1}H NMR (400 MHz, $CDCl_3$): δ 7.86-7.79 (m, 9H), 7.71-7.65 (m, 6H), 7.43-7.34 (m, 1H), 5.64 (d, J_{H-P} = 14.3 Hz, 2H). ^{13}C {^{1}H} NMR (101 MHz, $CDCl_3$): δ 146.8 (dm, J_{C-F} = 249.6 Hz), 146.3 (dm, J_{C-F} = 249.3 Hz), 140.4 (m, 2xC), 135.5 (d, J_{C-P} = 3.0 Hz, 3xC), 134.0 (d, J_{C-P} = 10.0 Hz, 6xC), 130.3 (d, J_{C-P} = 12.7 Hz, 6xC), 116.7 (d, J_{C-P} = 86.2 Hz, 3xC), 114.9 (d, J_{C-P} = 20.7 Hz), 111.9 (m), 24.0 (d, J_{C-P} = 50.0 Hz). ^{19}F {^{1}H} NMR (376 MHz, $CDCl_3$): δ -139.49 (ddt, *J* = 21.6, 12.5, 2.9 Hz, 1F), -142.46 (ddt, *J* = 20.4, 12.4, 3.9 Hz, 1F), -156.56 (m, 1F), -157.99 (tt, *J* = 20.5, 2.7 Hz, 1F). ^{31}P {^{1}H} NMR (162 MHz, $CDCl_3$): δ 23.51 (m, 1P). HRMS (APCI/TOF) *m/z*: M^+ Calcd for $C_{25}H_{18}PF_4$, 425.1077; Found 425.1075.

(*E*)-2-[2-(2,3,4,5-Tetrafluorophenyl)ethenyl]benzo[*c*]phenanthrene (10). Diisopropylamine (990 μL, 7.02 mmol, 1.2 eq) was dissolved in dry THF (200 mL) in a 500 mL round-bottom flask under argon atmosphere. The solution was cooled down to 0 °C and a solution of *n*-butyllithium (2.5M in hexanes, 2.58 mL, 1.1 eq) was added dropwise and stirred at 0 °C for an additional hour. The reaction mixture was then cooled down to -78 °C and (2,3,4,5-tetrafluorobenzyl)triphenylphosphonium bromide (**9**) (3.55 g, 7.02 mmol, 1.2 eq) was added dropwise and stirred for an hour. Then, benzo[*c*]phenantrene-2-carbaldehyde (**8**) (1.5 g, 5.85 mmol, 1 eq) was carefully added in a flow of argon and the mixture was heated up to 50 °C and stirred at the same temperature under argon overnight. Reaction was quenched with an addition of water (20 mL) and extracted with DCM (3 x 50 mL), dried over anhydrous $MgSO_4$, filtered through a short silica pad and dry-loaded to silica gel and purified by a column chromatography using petroleum ether as mobile phase to provide (*E*)-**10** (1.68 g, 71 %) as a white powder. mp 189.5-191.5 °C. ^{1}H NMR (400 MHz, $CDCl_3$): δ 8.95 (s, 1H), 8.64 (d, *J* = 8.5 Hz, 1H), 8.01 (dd, *J* = 7.9, 1.5 Hz, 1H), 7.93 – 7.80 (m, 5H), 7.62 (ddd, *J* = 8.0, 6.9, 1.1 Hz, 1H), 7.51 (ddd, *J* = 8.5, 6.9, 1.5 Hz, 1H), 7.45 (dd, *J* = 8.2, 1.6 Hz, 1H), 7.10 (d, *J* = 12.0 Hz, 1H), 6.99-6.91 (m, 1H), 6.62 (d, *J* = 12.0 Hz, 1H). ^{13}C {^{1}H} NMR was not observed due to a low solubility. ^{19}F {^{1}H} NMR (376 MHz, $CDCl_3$): δ -142.54 (m, 1F), -142.86 (m, 1F), -158.65 (m, 1F), -159.68 (m, 1F). IR (cm^{-1}): 1632, 1606, 1599, 1527, 1481, 1430, 1365, 1305, 1234, 1261, 1159, 1136, 1111, 1069, 963, 870, 809, 664, 621, 575, 437. EIMS *m/z*: 402 (100%, $M^{+\cdot}$), 382 (11%), 226 (13%). HRMS (APCI/TOF) *m/z*: M^+ Calcd for $C_{26}H_{14}F_4$, 402.1032; Found 402.1063.

(*E*)-4-[2-(2-Naphthalenyl)ethenyl]benzaldehyde (11). 250 mL round-bottomed flask was charged with (*E*)-2-[2-(4-bromophenyl)ethenyl]naphthalene (**i**) (2.0 g, 6.47 mmol, 1 eq) and dry THF (100 mL) was

added. Mixture was cooled down to -78 °C and a solution of *n*-butyllithium (2.5M in hexanes, 3.88 mL, 9.70 mmol, 1.5 eq) was slowly added. Reaction was allowed to stir for 3 hours at the same temperature and dry DMF (0.75 mL, 9.70 mmol, 1.5 eq) was added. After 2 hours, the reaction was allowed to warm up to rt and a saturated solution of NH_4Cl was used to quench the reaction. Organic volatiles were evaporated at reduced pressure. Water (50 mL) was added and the crude product was extracted with DCM (3 x 50 mL), dried over anhydrous $MgSO_4$, filtered through a short silica pad and dry-loaded to silica gel and purified by a column chromatography using petroleum ether and DCM (2:1) as mobile phase to provide 0.65 g (39 %) of **11** as a yellow solid. mp 162-163 °C (lit.[51] mp 162-164 °C). ^{1}H NMR (400 MHz, $CDCl_3$): δ 10.01 (s, 1H), 7.91-7.82 (m, 6H), 7.77-7.70 (m, 3H), 7.51-7.48 (m, 2H), 7.44 (d, *J* = 16.1 Hz, 1H), 7.28 (d, *J* = 16.1 Hz, 1H) (in agreement with published data in lit.[83]).

2-[2-(4-(2-(2,3,4,5-Tetraflorophenyl)ethenyl)phenyl)ethenyl]naphthalene (12). 500 mL round-bottomed flask was charged with dry THF (200 mL) and diisopropylamine (0.76 mL, 5.42 mmol, 1.4 eq) under argon atmosphere. The mixture was cooled down to 0 °C and a solution of *n*-butyllithium (2.5M in hexanes, 2 mL, 5.03 mmol, 1.3 eq) was added dropwise and stirred at the same temperature for an hour. Then, the reaction mixture was cooled down to -78 °C and (2,3,4,5-tetrafluorobenzyl)triphenylphosphonium bromide (**9**) (2.34 g, 4.65 mmol, 1.2 eq) was carefully added in a flow of argon. After an hour, 4-[2-(2-naphthalenyl)ethenyl] benzaldehyde (**11**) (1.0 g, 3.87 mmol, 1 eq) was carefully added in a flow of argon and the reaction mixture was stirred at 50 °C under argon overnight. Reaction was quenched by an addition of water (20 mL) and extracted with DCM (3 x 50 mL), dried over anhydrous $MgSO_4$ and filtered through a short silica pad (DCM). The volume of solvent was reduced under *in vacuo* and the spontaneous crystallization provided **12** (1.15 g, 74 %) as a white powder, a mixture of (*E*,*E*)- and (*E*,*Z*)-isomer. ^{1}H NMR spectrum of (*E*,*Z*)-isomer was obtained via LC-^{1}H-NMR with acetonitrile/water (85:15) as mobile phase. mp 133.5-139.0 °C. ^{1}H NMR (400 MHz, $CDCl_3$): (*E*,*Z*) major δ 7.87-7.79 (m, 4H), 7.73 (d, *J* = 8.6, 1.6 Hz, 1H), 7.51 - 7.42 (m, 4H), 7.33-7.15 (m, 4H), 6.91 - 6.82 (m, 1H), 6.81 (d, *J* = 11.9 Hz, 1H), 6.47 (d, *J* = 11.9 Hz, 1H). ^{1}H NMR (500 MHz, CH_3CN/D_2O): (*E*,*Z*) δ 7.96 (s, 1H), 7.91 - 7.86 (m, 3H), 7.83 (d, *J* = 8.8 Hz, 1H), 7.55 - 7.47 (m, 4H), 7.40 (d, *J* = 16.5 Hz, 1H), 7.33 (d, *J* = 16.5, 1H), 7.24 (d, *J* = 8.2, 2H), 7.04 - 6.97 (m, 1H), 6.91 (d, *J* = 12.0 Hz, 1H), 6.52 (d, *J* = 12.0 Hz, 1H). ^{13}C {^{1}H} NMR was not observed due to a low solubility. ^{19}F {^{1}H} NMR (376 MHz, $CDCl_3$): (*E*,*E*) minor δ -142.86 (m, 1F), -147.25 (ddd, *J* = 20.1, 12.2, 2.2 Hz, 1F), -159.08 (m, 1F), -160.10 (m, 1F) ppm; (*E*,*Z*) major δ -142.90 (ddd, *J* = 21.2, 12.0, 2.1 Hz, 1F), -143.24 (ddd, *J* = 20.9, 12.2, 3.3 Hz, 1F), -159.03 (td, *J* = 20.1, 2.3 Hz, 1F), -159.77 (ddd, *J* = 22.1, 19.5, 2.8 Hz, 1F). IR (cm^{-1}): 3060, 3032, 1633 (CH=CH), 1621, 1602, 1572, 1524, 1511, 1479, 1405, 1326, 1275, 1242, 1185, 1049, 961, 934, 829. EIMS *m/z*: 404 (100%, $M^{+\cdot}$), 228 (16%). HRMS (APCI/TOF) *m/z*: M^+ Calcd for $C_{26}H_{16}F_4$, 404.1188; Found 404.1179.

2,7-Naphthalenedicarbaldehyde (13). 2,7-Dibromonaphtalene (3 g, 10.50 mmol, 1 eq) was dissolved in

dry THF (100 mL) under argon in a 250 mL round-bottomed flask. The mixture was cooled down to -78 °C and a solution of *tert*-butyllithium (1.9M in pentane, 28.7 mL, 5.2 eq) was added dropwise and allowed to stir for an hour at the same temperature. DMF (4 mL, 52 mmol, 5 eq) was added and the mixture was stirred at the same temperature for 30 min and then allowed to heat up to room temperature (30 min) then it was quenched by an addition of aqueous 10% HCl (10 mL). Solvents were removed and the crude product was extracted with DCM (3 x 80 mL). Combined organic fractions were dried over anhydrous $MgSO_4$, filtered through a short silica pad and evaporated to dryness. The residue was dry loaded onto silica gel and purified by a column chromatography with petroleum ether/ethyl acetate (10:1) as mobile phase to provide **13** (1.74 g, 90 %) as a white solid after spontaneous crystallization. mp 144-146°C (petroleum ether-ethyl acetate); (lit.[84] mp 145-146 °C / DCM). ^{1}H NMR (400 MHz, $CDCl_3$): δ 10.23 (s, 2H), 8.52 (s, 2H), 8.12 (dd, *J* = 8.5, 1.5 Hz, 2H) 8.03 (d, *J* = 8.5 Hz, 2H) (in agreement with published data in lit.[84]).

2,7-Bis[2-(2,3,4,5-tetrafluorophenyl)ethenyl]naphthalene (14). 500 mL round-bottomed flask was charged with dry THF (200 mL) and diisopropylamine (2.2 mL, 15.64 mmol, 2.4 eq) under argon atmosphere. The mixture was cooled down to 0 °C and a solution of *n*-butyllithium (2.5M in hexanes, 5.73 mL, 2.2 eq) was added dropwise and stirred at the same temperature for an hour. Then, the reaction mixture was cooled down to -78 °C and (2,3,4,5-tetrafluorobenzyl)triphenyl phosphonium bromide (**9**) (7.9 g, 15.64 mmol, 2.4 eq) was carefully added in a flow of argon. After an hour, 2,7-naphthalenedicarbaldehyde (**13**) (1.2 g, 6.51 mmol, 1.0 eq was carefully added in a flow of argon and the reaction mixture was stirred at 50 °C under argon overnight. Reaction was quenched by an addition of water (20 mL) and extracted with DCM (3 x 75 mL), dried over anhydrous $MgSO_4$, filtered through a short silica pad and evaporated to dryness. The residue was dry loaded onto silica gel and purified by a column chromatography with petroleum ether as a mobile phase to provide **14** (3.0 g, 97 %) as a white powder, a mixture of isomers. ^{1}H NMR spectra were obtained for all three (*E*,*E*)/(*E*,*Z*)/(*Z*,*Z*)-isomers via LC-^{1}H-NMR with acetonitrile/water (85:15) as mobile phase. mp 98.5-103.5 °C. ^{1}H NMR (500 MHz, CH_3CN/D_2O): (*Z*,*Z*) δ 7.67 (d, *J* = 8.5 Hz, 2H), 7.53 (s, 2H), 7.24 (d, *J* = 8.5 Hz, 2H), 6.96 (d, *J* = 11.9 Hz, 2H), 6.91-6.85 (m, 2H), 6.53 (d, *J* = 11.9 Hz, 2H) ppm; (*E*,*Z*) δ 7.85-7.71 (m, 3H) 7.69 (s, 1H) 7.51-7.45 (m, 1H), 7.37 (d, *J* = 16.2 Hz, 1H), 7.27 (m, 1H), 7.01 (d, *J* = 12.2 Hz, 1H), 6.95-6.89 (m, 2H), 6.57 (d, *J* = 12.2 Hz, 2H) ppm; (*E*,*E*) δ 7.98 (s, 2H), 7.87 (d, *J* = 8.5 Hz, 2H), 7.79 (d, *J* = 8.5 Hz, 2H), 7.53-7.48 (m, 2H), 7.42 (d, *J* = 16.5 Hz, 2H), 7.32 (d, *J* = 16.5 Hz, 2H). ^{13}C {^{1}H} NMR was not observed due to a low solubility. ^{19}F {^{1}H} NMR (376 MHz, $CDCl_3$): δ (*Z*,*Z*) major -142.86 (ddd, *J* = 21.0, 12.4, 2.2 Hz, 2F), -143.20 (ddd, *J* = 20.7, 12.1, 3.1 Hz, 2F), -158.94 (td, *J* = 20.4, 2.4 Hz, 2F), -159.48 (td, *J* = 20.3, 3.1 Hz, 2F). IR (cm^{-1}): 1637 (CH=CH), 1621, 1599, 1562, 1523, 1479, 1432, 1310, 1273, 1245, 1239, 1133, 1160, 956, 926, 911, 853, 615, 584, 436. EIMS *m/z*: 476 (100%, $M^{+\cdot}$), 456 (11%), 436 (13%), 300 (16%). HRMS (APCI/TOF) *m/z*: M^+ Calcd for $C_{26}H_{12}F_8$, 476.0811; Found 476.0817.

1,2,3,4,13,14,15,16-Octafluoro[6]helicene (15). 2,7-Bis[2-(2,3,4,5-tetrafluorophenyl)ethenyl]naphthalene (**14**) (1.0 g, 2.1 mmol, 1 eq) and iodine (0.2 g, 0.79 mmol, 0.16 eq) were dissolved in toluene (2 L) and subjected to the photoreaction in a continuous flow setup (see chapter 1.2.2.) with a flow rate of 50 mL.min-1. Reaction mixture was washed through an in-line column packed with silica gel (30 g) and sodium thiosulfate (50 g) to remove the excess iodine and insoluble byproducts. Solvent was removed under reduced pressure and a recrystallization from hot toluene provided **15** (0.31 g, 78 %) as yellow crystals. ^{1}H NMR (400 MHz, C_6D_6): δ 7.82 (d, *J* = 8.8 Hz, 2H), 7.73 (d, *J* = 8.2 Hz, 2H), 7.60 (d, *J* = 8.2 Hz, 2H), 7.50 (d, *J* = 8.8 Hz, 2H). ^{13}C {^{1}H} NMR (126 MHz, $C_2D_2Cl_4$, 95 °C): δ 131.9, 131.0, 128.0, 127.6, 127.0, 124.8, 123.1, 118.4 (m), 118.0, 115.0 (Other quaternary carbons interacting with fluorine nuclei were not detected). ^{19}F {^{1}H} NMR (376 MHz, $CDCl_3$): δ -135.06 (m, 2F), -151.73 (dd, *J* = 20.4, 12.9 Hz, 2F), -161.25 (td, *J* = 20.4, 4.1 Hz, 2F), -162.71 (t, *J* = 20.1 Hz, 2F). IR (cm^{-1}): 1654, 1522, 1497, 1273, 1184, 1013, 957, 649, 579. EIMS *m/z*: 472 (100%, $M^{+\cdot}$), 452 (12%), 403 (20%), 372 (29%). HRMS (APCI/TOF) *m/z*: M^+ Calcd for $C_{26}H_8F_8$ 472.0498; found 472.0490. Sublimation Point: 329 °C (760 mmHg).

(*E*)-2-[2-(4-Bromophenyl)ethenyl]naphthalene (i). Sodium hydride (60% in mineral oil, 0.27 g, 6.7 mmol, 1.05 eq) was charged into round-bottomed flask and dry THF (50 mL) was added. Into the suspension, diethyl 4-bromobenzylphosphonate[85] (2.06 g, 6.7 mmol, 1.05 eq) was added dropwise and stirred for 10 minutes. A solution of 2-napthaldehyde (1.0 g, 6.4 mmol, 1 eq in 30 mL of dry THF) was added dropwise. Mixture was heated up to 50 °C and stirred overnight. Reaction was quenched with addition of water (100 mL) and THF was evaporated. Precipitate was filtered out, dissolved in DCM (50 mL), dried over anhydrous magnesium sulfate and filtered through a silica pad (DCM). Solvents were evaporated and residual volatiles removed under high vacuum yielding the desired intermediate (*E*)-(**i**) (1.65 g, 83%) as a white powder. mp 187-188 °C (methanol); (lit.[86] mp 188.5-189 °C / acetone). ^{1}H NMR (400 MHz, $CDCl_3$): δ 7.89−7.79 (m, 4H), 7.73 (dd, *J* = 8.7 Hz, 1.7 Hz, 1H), 7.53−7.40 (m, 6H), 7.27 (d, *J* = 16.3 Hz, 1H), 7.16 (d, *J* = 16.3 Hz, 1H) (in agreement with published data in lit.[19,86]).

2-Bromobenzo[*c*]phenanthrene (ii). (*E*)-2-[2-(4-Bromophenyl)ethenyl]naphthalene (**i**) (4.0 g, 13 mmol, 1 eq) and iodine (330 mg, 1.3 mmol, 0.1 eq) were dissolved in 4 L of toluene. The reaction mixture was subjected to the photoreaction in a continuous flow setup (see chapter 1.2.2.) with a flow rate of 50 mL.min-1. After the completion of photoreaction, reaction mixture was washed through the layer of sodium thiosulfate (50 g) and silica gel (30 g) using toluene. Solvent was removed under reduced pressure and the crude product was recrystallized from hot methanol to provide the desired intermediate (**ii**) (2.43 g, 61%) as white crystals. The mother liquor was evaporated to dryness and purified by column chromatography using 30:1 hexane/ethyl acetate yielding additional (**ii**) (1.07 g, 27%). The overall yield of the reaction was 3.50 g (88%) of (**ii**). mp 87-88 °C; (lit.[86] mp 86-88 °C). ^{1}H NMR (400 MHz, $CDCl_3$): δ 9.29 (d, *J* = 1.8 Hz,

1 H), 9.05 (d, *J* = 8.5 Hz, 1H), 8.03 (dd, *J* = 7.9, 1.4 Hz, 1H), 7.93 (d, *J* = 8.5 Hz, 1H), 7.89 (d, *J* = 8.5 Hz, 1H), 7.86−7.85 (m, 2H), 7.82 (d, *J* = 8.5 Hz, 1H), 7.74 (ddd, *J* = 6.9, 6.9, 1.5 Hz, 1H), 7.71 (dd, *J* = 6.7, 1.9 Hz, 1H), 7.66 (ddd, *J* = 6.9, 6.9, 1.2 Hz, 1H) (in agreement with published data in lit.[19,86]). HRMS (APCI/TOF) *m/z*: $[M+H]^+$ Calcd for $C_{18}H_{12}Br$, 307.0116 ($[M+H]^+$); Found 307.0115.

2,3,4,5-Tetrafluorobenzylalcohol (iii). A suspension of sodium tetrahydroborate (1.1 g, 29 mmol, 1.4 eq) in dry THF (100 mL) was prepared under argon in 250 mL round-bottom flask. A solution of 2,3,4,5-tetrafluorobenzoic acid (4.0 g, 20.1 mmol, 1.0 eq) in dry THF (50 mL) was added dropwise and stirred until the gas evolution stopped. The solution of iodine (2.88 g, 11.35 mmol, 0.55 eq) in dry THF (20 mL) was added dropwise. The reaction mixture was stirred at 55 °C overnight under condenser, then it was quenched by an addition of MeOH (10 mL). Solvents were removed under reduced pressure and the crude reaction product was dissolved in DCM (100 mL), washed through a silica pad (DCM) and evaporated to dryness. The vacuum distillation at 82-85 °C (8 mmHg) provided (**iii**) **(**3.12 g, 84 %) as a yellowish oil. bp = 82-85 °C / 8 mmHg (lit.[87] (bp 132-134 °C / 60 mmHg). ^{1}H NMR (400 MHz, DMSO-d_6): δ 7.40-7.30 (m, 1H), 5.58 (t, *J* = 5.8 Hz, 1H), 4.55 (d, *J* = 5.8 Hz, 2H). ^{13}C {^{1}H} NMR (101 MHz, $CDCl_3$): δ 147.2 (dddd, J_{C-F} = 247.0, 10.1, 3.6, 2.1 Hz), 144.8 (dddd, J_{C-F} = 246.1, 10.5, 3.7, 1.5 Hz), 140.5 (dddd, J_{C-F} = 253.3, 16.4, 12.4, 3.8 Hz), 139.9 (dddd, J_{C-F} = 252.8, 16.7, 12.3, 3.5 Hz), 124.2 (ddd, J_{C-F} = 13.6, 6.3, 3.9 Hz), 109.7 (dt, J_{C-F} = 19.9, 3.9 Hz), 57.9 (t, J_{C-F} = 3.2 Hz). ^{19}F {^{1}H} NMR (376 MHz, $CDCl_3$): δ -142.29 (ddd, *J* = 21.1, 13.0, 2.6 Hz, 1F), -148.39 (ddd, *J* = 20.8, 13.0, 2.9 Hz, 1F), -159.13 (dt, *J* = 20.0, 2.3 Hz, 1F), -160.13 (ddd, *J* = 20.8, 19.4, 2.8 Hz, 1F). EIMS *m/z* 180 (100%, $M^{+\cdot}$), 163 (25%), 159 (100%), 151 (75%), 132 (50%). HRMS (APCI/TOF) *m/z*: detected as fluorinated tropylium cation (major peak): M^+ Calcd for $C_7H_3F_4^+$, 163.0165; Found 163.0168; product (minor peak): M^+ Calcd for $C_7H_4F_4O$, 180.0198; Found 180.0198.

2,3,4,5-Tetrafluorobenzylbromide (iv). 2,3,4,5-Tetrafluorobenzylalcohol (**iii**) (2.66 g, 14.8 mmol, 1 eq) was dissolved in dry Et_2O (50 mL) and cooled down to 0 °C. Phosphorus tribromide (4.40 g, 16.25 mmol, 1.1 eq) was added dropwise and the reaction mixture was kept at 0°C for 3 hours then slowly allowed to warp up to room temperature and stirred at the same temperature overnight. The reaction mixture was quenched by addition of water (5 mL) and extracted to Et_2O (3 x 25 mL), dried over anhydrous $MgSO_4$ and concentrated *in vacuo*. The vacuum distillation at 50 °C (4 mmHg) provided (**iv**) **(**3.35 g, 93 %) as a clear colorless liquid. Product (**iv**) was stored at 5 °C and protected from light. bp = 50 °C / 4 mmHg (lit.[87] bp 107-110 °C / 65 mmHg). ^{1}H NMR (400 MHz, $CDCl_3$): δ 7.04 (m, 1H), 4.43 (d, *J* = 1.4 Hz, 2H). ^{13}C {^{1}H} NMR (101 MHz, $CDCl_3$): δ 147.0 (dddd, J_{C-F} = 248.1, 10.2, 3.7, 2.4 Hz), 145.7 (dddd, J_{C-F} = 250.2, 10.8, 3.7, 1.5 Hz), 142.2 – 141.7 (m), 139.7 – 139.2 (m), 121.6 (m), 112.1 (dt, *J* = 19.9, 3.1 Hz), 23.3 (m). ^{19}F {^{1}H} NMR (376 MHz, $CDCl_3$): δ -141.44 (ddd, *J* = 20.9, 12.5, 2.6 Hz, 1F), -144.69 (ddd, *J* = 19.8, 12.5,

4.1 Hz, 1F), -157.31 (ddd, *J* = 20.9, 19.8, 4.1 Hz, 1F), -157.63 (td, *J* = 19.8, 2.6 Hz, 1F). EIMS *m/z*: 244 (5%), 242 (5%, $M^{+\cdot}$), 163 (100%), 143 (25%). HRMS (APCI/TOF) *m/z*: n.d. (decomposition). HRMS (EI/TOF) *m/z*: $[M]^+$ Calcd for $C_7H_3F_4Br$, 241.9353 ($[M+H]^+$); Found 241.9354.

AUTHOR INFORMATION

Corresponding Authors

*cirkva@icpf.cas.cz

*sykora@icpf.cas.cz

*jan.vacek@upol.cz

ORCID

Vladimír Církva: 0000-0001-5351-4003

Jan Hrbáč: 0000-0002-1079-4276

Pavel Jakubík: 0000-0001-5079-0555

Jan Storch: 0000-0002-1970-8485

Tomáš Strašák: 0000-0001-6413-0494

Jan Sýkora: 0000-0002-2930-8880

Jan Vacek: 0000-0001-5490-082X

Ivana Císařová: 0000-0002-9612-9831

Jaroslav Žádný: 0000-0002-3737-3519

SUPPORTING INFORMATION

Setup of photoreactions, X-ray crystallography details, separation of enantiomers and racemization barrier determination, DFT Calculations details, ^1H, ^{19}F, ^{13}C, ^{31}P NMR spectra.

ACKNOWLEDGMENTS

This work was supported by the Czech Science Foundation, (V.C., grant No. 17-02578S, synthetic part, J. Sýkora, I.C.: grant No. 15-12719S, NMR, DFT and X-ray study) and the Czech Ministry of Education, Youth and Sports (J.V., RVO: 61989592, electrochemical studies). The authors are grateful to Andrew Christensen for proof reading.

Keywords

Fluorohelicenes, flow reactor, photocyclization, enantiomer, optical properties

REFERENCES

(1) Wynberg, H. Some Observations on the Chemical, Photochemical, and Spectral Properties of Thiophenes. *Acc. Chem. Res.* **1971**, *4* (2), 65–73.

(2) Martin, R. H. The Helicenes. *Angew. Chemie Int. Ed.* **1974**, *13* (10), 649–660.

(3) Chen, C.-F.; Shen, Y. *Helicene Chemistry*; Springer: Berlin, Heidelberg, 2017.

(4) Laarhoven, W. H.; Prinsen, W. J. C. Carbohelicenes and Heterohelicenes. *Top. Curr. Chem.* **1984**, *125*, 63–130.

(5) Meurer, K. P.; Vögtle, F. Helical Molecules in Organic Chemistry. In *Topics in Current Chemistry*; Springer-Verlag: Berlin/Heidelberg, 1985; Vol. 127, pp 1–76.

(6) Urbano, A. Recent Developments in the Synthesis of Helicene-Like Molecules. *Angew. Chemie Int. Ed.* **2003**, *42* (34), 3986–3989.

(7) Stará, I. G.; Starý, I. Vol. 45b. In *Aromatic ring assemblies, polycyclic aromatic hydrocarbons, and conjugated polyenes*; Siegel, J. S., Tobe, Y., Eds.; Thieme: Stuttgart, 2010; p 885.

(8) Shen, Y.; Chen, C. Helicenes: Synthesis and Applications. *Chem. Rev.* **2012**, *112* (3), 1463–1535.

(9) Gingras, M. One Hundred Years of Helicene Chemistry. Part 1: Non-Stereoselective Syntheses of Carbohelicenes. *Chem. Soc. Rev.* **2013**, *42* (3), 968–1006.

(10) Gingras, M.; Félix, G.; Peresutti, R. One Hundred Years of Helicene Chemistry. Part 2: Stereoselective Syntheses and Chiral Separations of Carbohelicenes. *Chem. Soc. Rev.* **2013**, *42* (3), 1007–1050.

(11) Gingras, M. One Hundred Years of Helicene Chemistry. Part 3: Applications and Properties of Carbohelicenes. *Chem. Soc. Rev.* **2013**, *42* (3), 1051–1095.

(12) Newman, M. S.; Lednicer, D. The Synthesis and Resolution of Hexahelicene. *J. Am. Chem. Soc.* **1956**, *78* (18), 4765–4770.

(13) Jutz, C.; Löbering, H.-G. A Novel Simple Synthesis of Helicenes. *Angew. Chemie Int. Ed.* **1975**, *14* (6), 418–420.

(14) Teplý, F.; Stará, I. G.; Starý, I.; Kollárovič, A.; Šaman, D.; Rulíšek, L.; Fiedler, P. Synthesis of [5]-, [6]-, and [7]Helicene via Ni(0)- or Co(I)-Catalyzed Isomerization of Aromatic cis, cis -Dienetriynes. *J. Am. Chem. Soc.* **2002**, *124* (31), 9175–9180.

(15) Collins, S. K.; Grandbois, A.; Vachon, M. P.; Côté, J. Preparation of Helicenes through Olefin Metathesis. *Angew. Chemie Int. Ed.* **2006**, *45* (18), 2923–2926.

(16) Stará, I. G.; Andronova, A.; Kollárovič, A.; Vyskočil, Š.; Jugé, S.; Lloyd-Jones, G. C.; Guiry, P. J.; Starý, I. Enantioselective [2+2+2] Cycloisomerisation of Alkynes in the Synthesis of Helicenes: The Search for Effective Chiral Ligands. *Collect. Czechoslov. Chem. Commun.* **2011**, *76* (12), 2005–2022.

(17) Žádný, J.; Velíšek, P.; Jakubec, M.; Sýkora, J.; Církva, V.; Storch, J. Exploration of 9-Bromo[7]Helicene Reactivity. *Tetrahedron* **2013**, *69* (30), 6213–6218.

(18) Mohamed, R. K.; Mondal, S.; Guerrera, J. V.; Eaton, T. M.; Albrecht-Schmitt, T. E.; Shatruk, M.;

Alabugin, I. V. Alkynes as Linchpins for the Additive Annulation of Biphenyls: Convergent Construction of Functionalized Fused Helicenes. *Angew. Chemie Int. Ed.* **2016**, *55* (39), 12054–12058.

(19) Jakubec, M.; Beránek, T.; Jakubík, P.; Sýkora, J.; Žádný, J.; Církva, V.; Storch, J. 2-Bromo[6]Helicene as a Key Intermediate for [6]Helicene Functionalization. *J. Org. Chem.* **2018**, *83* (7), 3607–3616.

(20) Talele, H. R.; Chaudhary, A. R.; Patel, P. R.; Bedekar, A. V. Expeditious Synthesis of Helicenes Using an Improved Protocol of Photocyclodehydrogenation of Stilbenes. *Arkivoc* **2011**, *2011* (9), 15.

(21) Nakai, Y.; Mori, T.; Inoue, Y. Theoretical and Experimental Studies on Circular Dichroism of Carbo[n]Helicenes. *J. Phys. Chem. A* **2012**, *116* (27), 7372–7385.

(22) Církva, V. Microwaves in Photochemistry and Photocatalysis. In *Microwaves in Organic Synthesis*; Wiley-VCH Verlag GmbH & Co. KGaA: Weinheim, Germany, 2012; pp 563–605.

(23) Storch, J.; Církva, V.; Bernard, M.; Vokál, J. Process for Preparing [6]Helicenes by Photocyclization. CZ303997, 2013.

(24) Hoffmann, N. Photochemical Reactions Applied to the Synthesis of Helicenes and Helicene-like Compounds. *J. Photochem. Photobiol. C Photochem. Rev.* **2014**, *19* (1), 1–19.

(25) Li, Z.; Twieg, R. J. Photocyclodehydrofluorination. *Chem. - A Eur. J.* **2015**, *21* (44), 15534–15539.

(26) Matsushima, T.; Kobayashi, S.; Watanabe, S. Air-Driven Potassium Iodide-Mediated Oxidative Photocyclization of Stilbene Derivatives. *J. Org. Chem.* **2016**, *81* (17), 7799–7806.

(27) Martin, R. H.; Flammang-Barbieux, M.; Cosyn, J. P.; Gelbcke, M. 1-Synthesis of Octa- and Nonahelicenes. 2-New Syntheses of Hexa- and Heptahelicenes. 3-Optical Rotation and O.R.D. of Heptahelicene. *Tetrahedron Lett.* **1968**, *9* (31), 3507–3510.

(28) Martin, R. H.; Marchant, M.; Baes, M. Rapid Syntheses of Hexa and Heptahelicene. *Helv. Chim. Acta* **1971**, *54* (1), 358–360.

(29) Kagan, H.; Moradpour, A.; Nicoud, J. F.; Balavoine, G.; Tsoucaris, G. Photochemistry with Circularly Polarized Light. Synthesis of Optically Active Hexahelicene. *J. Am. Chem. Soc.* **1971**, *93* (9), 2353–2354.

(30) Moradpour, A.; Kagan, H.; Baes, M.; Morren, G.; Martin, R. H. Photochemistry with Circularly Polarized Light—III. *Tetrahedron* **1975**, *31* (17), 2139–2143.

(31) Mallory, F. B.; Mallory, C. W. Photocyclization of Stilbenes and Related Molecules. *Org. React.* **1984**, *30*, 1–456.

(32) Prinsen, W. J. C.; Laarhoven, W. H. Formation of 5,6- and 7,8-Dihydrohexahelicene: Mechanistic Details of the Rearrangement of the Primary Photocyclization Product of 2-Styrylbenzo[c]Phenanthrene in the Presence of a Base. *J. Org. Chem.* **1989**, *54* (15), 3689–3694.

(33) Liu, L.; Yang, B.; Katz, T. J.; Poindexter, M. K. Improved Methodology for Photocyclization Reactions. *J. Org. Chem.* **1991**, *56* (12), 3769–3775.

(34) Talele, H. R.; Gohil, M. J.; Bedekar, A. V. Synthesis of Derivatives of Phenanthrene and Helicene by Improved Procedures of Photocyclization of Stilbenes. *Bull. Chem. Soc. Jpn.* **2009**, *82* (9), 1182–1186.

(35) Sakamoto, Y.; Suzuki, T.; Kobayashi, M.; Gao, Y.; Fukai, Y.; Inoue, Y.; Sato, F.; Tokito, S. Perfluoropentacene: High-Performance p−n Junctions and Complementary Circuits with

Pentacene. *J. Am. Chem. Soc.* **2004**, *126* (26), 8138–8140.

(36) Rasmusson, T.; Martyn, L. J. P.; Chen, G.; Lough, A.; Oh, M.; Yudin, A. K. Aromatic Fluorine as a Versatile Control Element for the Construction of Molecules with Helical Chirality. *Angew. Chemie Int. Ed.* **2008**, *47* (37), 7009–7012.

(37) Brooke, G. M. The Preparation and Properties of Polyfluoro Aromatic and Heteroaromatic Compounds. *J. Fluor. Chem.* **1997**, *86* (1), 1–76.

(38) Hiyama, T. *Organofluorine Compounds*; Yamamoto, H., Ed.; Springer Berlin Heidelberg: Berlin, Heidelberg, 2000.

(39) Chambers, R. D. Fluorine in Organic Chemistry. In *Fluorine in Organic Chemistry*; Blackwell Publishing Ltd.: Oxford, UK, 2004; p 296.

(40) Uneyama, K. *Organofluorine Chemistry*; Uneyama, K., Ed.; Blackwell Publishing: Oxford, UK, 2006.

(41) Amii, H.; Uneyama, K. C−F Bond Activation in Organic Synthesis. *Chem. Rev.* **2009**, *109* (5), 2119–2183.

(42) Banerjee, S.; Sinha, S.; Pradhan, P.; Caruso, A.; Liebowitz, D.; Parrish, D.; Rossi, M.; Zajc, B. Regiospecifically Fluorinated Polycyclic Aromatic Hydrocarbons via Julia–Kocienski Olefination and Oxidative Photocyclization. Effect of Fluorine Atom Substitution on Molecular Shape. *J. Org. Chem.* **2016**, *81* (10), 3983–3993.

(43) Liang, T.; Neumann, C. N.; Ritter, T. Introduction of Fluorine and Fluorine-Containing Functional Groups. *Angew. Chemie Int. Ed.* **2013**, *52* (32), 8214–8264.

(44) Cozzi, F.; Bacchi, S.; Filippini, G.; Pilati, T.; Gavezzotti, A. Synthesis, X-Ray Diffraction and Computational Study of the Crystal Packing of Polycyclic Hydrocarbons Featuring Aromatic and Perfluoroaromatic Rings Condensed in the Same Molecule: 1,2,3,4-Tetrafluoronaphthalene, -anthracene and -phenanthrene. *Chem. - A Eur. J.* **2007**, *13* (25), 7177–7184.

(45) Li, H.; He, K.-H.; Liu, J.; Wang, B.-Q.; Zhao, K.-Q.; Hu, P.; Shi, Z.-J. Straightforward Synthesis of Phenanthrenes from Styrenes and Arenes. *Chem. Commun.* **2012**, *48* (56), 7028.

(46) Lemal, D. M. Cycloaddition Chemistry of Tetrafluorothiophene S,S-Dioxide. *J. Org. Chem.* **2016**, *81* (12), 4931–4938.

(47) Morrison, D. J.; Trefz, T. K.; Piers, W. E.; McDonald, R.; Parvez, M. 7:8,9:10-Dibenzo-1,2,3,4-Tetrafluorotriphenylene: Synthesis, Structure, and Photophysical Properties of a Novel [5]Helicene. *J. Org. Chem.* **2005**, *70* (13), 5309–5312.

(48) Cho, D. M.; Parkin, S. R.; Watson, M. D. Partial Fluorination Overcomes Herringbone Crystal Packing in Small Polycyclic Aromatics. *Org. Lett.* **2005**, *7* (6), 1067–1068.

(49) Amsharov, K. Y.; Kabdulov, M. A.; Jansen, M. Homo-Elimination of HF-An Efficient Approach for Intramolecular Aryl-Aryl Coupling. *Chem. - A Eur. J.* **2010**, *16* (20), 5868–5871.

(50) Papagni, A.; Buttero, P. Del; Bertarelli, C.; Miozzo, L.; Moret, M.; Pryce, M. T.; Rizzato, S. Novel Fluorinated Amino-Stilbenes and Their Solid-State Photodimerization. *New J. Chem.* **2010**, *34* (11), 2612.

(51) Bosiak, M. J.; Rakowiecki, M.; Orłowska, K. J.; Kędziera, D.; Adams, J. Synthesis and Photoluminescent Properties of Conjugated Aryl-Vinyl Dioctyl 2,6-Dimethylbenzofuro[5,6-b]Furan-3,7-Dicarboxylate Derivatives. *Dye. Pigment.* **2013**, *99* (3), 803–811.

(52) Dračínský, M.; Storch, J.; Církva, V.; Císařová, I.; Sýkora, J. Internal Dynamics in Helical

Molecules Studied by X-Ray Diffraction, NMR Spectroscopy and DFT Calculations. *Phys. Chem. Chem. Phys.* **2017**, *19* (4), 2900–2907.

(53) Ben Braiek, M.; Aloui, F.; Ben Hassine, B. Synthesis and Resolution of 2-Hydroxyhexahelicene. *Tetrahedron Lett.* **2013**, *54* (5), 424–426.

(54) Vander Donckt, E.; Nasielski, J.; Greenleaf, J. R.; Birks, J. B. Fluorescence of the Helicenes. *Chem. Phys. Lett.* **1968**, *2* (6), 409–410.

(55) Birks, J. B.; Birch, D. J. S.; Cordemans, E.; Vander Donckt, E. Fluorescence of the Higher Helicenes. *Chem. Phys. Lett.* **1976**, *43* (1), 33–36.

(56) Storch, J.; Zadny, J.; Strasak, T.; Kubala, M.; Sykora, J.; Dusek, M.; Cirkva, V.; Matejka, P.; Krbal, M.; Vacek, J. Synthesis and Characterization of a Helicene-Based Imidazolium Salt and Its Application in Organic Molecular Electronics. *Chem. - A Eur. J.* **2015**, *21* (6), 2343–2347.

(57) Vacek, J.; Hrbáč, J.; Strašák, T.; Církva, V.; Sýkora, J.; Fekete, L.; Pokorný, J.; Bulíř, J.; Hromadová, M.; Crassous, J.; Storch, J. Anodic Deposition of Enantiopure Hexahelicene Layers. *ChemElectroChem* **2018**, *5* (15), 2080–2088.

(58) D'Andrade, B. W.; Datta, S.; Forrest, S. R.; Djurovich, P.; Polikarpov, E.; Thompson, M. E. Relationship between the Ionization and Oxidation Potentials of Molecular Organic Semiconductors. *Org. Electron.* **2005**, *6* (1), 11–20.

(59) Hrbac, J.; Storch, J.; Halouzka, V.; Cirkva, V.; Matejka, P.; Vacek, J. Immobilization of Helicene onto Carbon Substrates through Electropolymerization of [7]Helicenyl-Thiophene. *RSC Adv.* **2014**, *4* (86), 46102–46105.

(60) Hrbáč, J.; Strašák, T.; Fekete, L.; Ladányi, V.; Pokorný, J.; Bulíř, J.; Krbal, M.; Žádný, J.; Storch, J.; Vacek, J. Potential-Driven On/Off Switch Strategy for the Electrosynthesis of [7]Helicene-Derived Polymers. *ChemElectroChem* **2017**, *4* (12), 3047–3052.

(61) Rulíšek, L.; Exner, O.; Cwiklik, L.; Jungwirth, P.; Starý, I.; Pospíšil, L.; Havlas, Z. On the Convergence of the Physicochemical Properties of [n]Helicenes. *J. Phys. Chem. C* **2007**, *111* (41), 14948–14955.

(62) Miyasaka, M.; Pink, M.; Olankitwanit, A.; Rajca, S.; Rajca, A. Band Gap of Carbon–Sulfur [n]Helicenes. *Org. Lett.* **2012**, *14* (12), 3076–3079.

(63) Bédard, A. C.; Vlassova, A.; Hernandez-Perez, A. C.; Bessette, A.; Hanan, G. S.; Heuft, M. A.; Collins, S. K. Synthesis, Crystal Structure and Photophysical Properties of Pyrene-Helicene Hybrids. *Chem. - A Eur. J.* **2013**, *19* (48), 16295–16302.

(64) Storch, J.; Kalíková, K.; Tesařová, E.; Maier, V.; Vacek, J. Development of Separation Methods for the Chiral Resolution of Hexahelicenes. *J. Chromatogr. A* **2016**, *1476*, 130–134.

(65) Martin, R. H.; Marchant, M. J. Thermal Racemisation of Hepta-, Octa-, and Nonahelicene. *Tetrahedron* **1974**, *30* (2), 347–349.

(66) Martin, R. H.; Marchant, M.-J. Thermal Racemisation of [6], [7], [8] and [9] Helicene. *Tetrahedron Lett.* **1972**, *13* (35), 3707–3708.

(67) Borkent, J. H.; Laarhoven, W. H. The Thermal Racemization of Methyl-Substituted Hexahelicenes. *Tetrahedron* **1978**, *34* (16), 2565–2567.

(68) Rickhaus, M.; Mayor, M.; Juríček, M. Strain-Induced Helical Chirality in Polyaromatic Systems. *Chem. Soc. Rev.* **2016**, *45* (6), 1542–1556.

(69) Ravat, P.; Hinkelmann, R.; Steinebrunner, D.; Prescimone, A.; Bodoky, I.; Juríček, M.

Configurational Stability of [5]Helicenes. *Org. Lett.* **2017**, *19* (14), 3707–3710.

(70) Lin, W.-B.; Li, M.; Fang, L.; Shen, Y.; Chen, C.-F. Synthesis, Structures, Resolution, and Chiroptical Properties of 1,16-Diaryl-Substituted Benzo[5]Helicene Derivatives. *Chem. - An Asian J.* **2017**, *12* (1), 86–94.

(71) Green, B. S.; Knossow, M. Lamellar Twinning Explains the Nearly Racemic Composition of Chiral, Single Crystals of Hexahelicene. *Science* **1981**, *214* (4522), 795–797.

(72) Lightner, D. A.; Hefelfinger, D. T.; Powers, T. W.; Frank, G. W.; Trueblood, K. N. Hexahelicene. Absolute Configuration. *J. Am. Chem. Soc.* **1972**, *94* (10), 3492–3497.

(73) Sýkora, J.; Beránek, T.; Císařová, I. *CCDC 1862806: Experimental Crystal Structure Determination*; 2018, DOI: 10.5517/ccdc.csd.cc20jdjh.

(74) Böhm, V. P. W.; Herrmann, W. A. Mechanism of the Heck Reaction Using a Phosphapalladacycle as the Catalyst: Classical versus Palladium(IV) Intermediates. *Chem. - A Eur. J.* **2001**, *7* (19), 4191–4197.

(75) Smallcombe, S. H.; Patt, S. L.; Keifer, P. A. WET Solvent Suppression and Its Applications to LC NMR and High-Resolution NMR Spectroscopy. *J. Magn. Reson. Ser. A* **1995**, *117* (2), 295–303.

(76) Sheldrick, G. M. SHELXT – Integrated Space-Group and Crystal-Structure Determination. *Acta Crystallogr. Sect. A Found. Adv.* **2015**, *71* (1), 3–8.

(77) Betteridge, P. W.; Carruthers, J. R.; Cooper, R. I.; Prout, K.; Watkin, D. J. CRYSTALS Version 12: Software for Guided Crystal Structure Analysis. *J. Appl. Crystallogr.* **2003**, *36* (6), 1487–1487.

(78) Sheldrick, G. M. SHELXL97. Program for Crystal Structure Refinement. University of Göttingen: Göttingen, Germany 1997.

(79) Sheldrick, G. M. Crystal Structure Refinement with SHELXL. *Acta Crystallogr. Sect. C Struct. Chem.* **2015**, *71* (1), 3–8.

(80) Farrugia, L. J. ORTEP-3 for Windows - A Version of ORTEP-III with a Graphical User Interface (GUI). *J. Appl. Crystallogr.* **1997**, *30* (5), 565.

(81) Frigoli, M.; Moustrou, C.; Samat, A.; Guglielmetti, R. Synthesis of New Thiophene-Substituted 3,3-Diphenyl-3H-Naphtho[2,1-b]Pyrans by Cross-Coupling Reactions, Precursors of Photomodulated Materials. *Eur. J. Org. Chem.* **2003**, No. 15, 2799–2812.

(82) Laarhoven, W. H.; Veldhuis, R. G. M. Conformational Studies on Hexahelicenes-II. Synthesis and Spectral Properties of Alkyl Hexahelicenes. *Tetrahedron* **1972**, *28* (6), 1811–1822.

(83) Luo, T.; Zhang, R.; Zhang, W.; Shen, X.; Umemoto, T.; Hu, J. Divergent Rearrangements of Cyclopropyl-Substituted Fluoroepoxides Involving C-F Bond Cleavage and Formation. *Org. Lett.* **2014**, *16* (3), 888–891.

(84) Granzhan, A.; Largy, E.; Saettel, N.; Teulade-Fichou, M. P. Macrocyclic DNA-Mismatch-Binding Ligands: Structural Determinants of Selectivity. *Chem. - A Eur. J.* **2010**, *16* (3), 878–889.

(85) Sontag, S. K.; Sheppard, G. R.; Usselman, N. M.; Marshall, N.; Locklin, J. Surface-Confined Nickel Mediated Cross-Coupling Reactions: Characterization of Initiator Environment in Kumada Catalyst-Transfer Polycondensation. *Langmuir* **2011**, *27* (19), 12033–12041.

(86) Brooks, M. A.; Scott, L. T. 1,2-Shifts of Hydrogen Atoms in Aryl Radicals. *J. Am. Chem. Soc.* **1999**, *121* (23), 5444–5449.

(87) Petrova, T. D.; Savchenko, T. I.; Kukovinets, O. S.; Yakobson, G. G. Polyfluorinated Heterocyclic

Compounds XI. About the Formation of Trifluoroindoles from β-Tetrafluorophenylethylamines. *Izv. Sib. Otd. Akad. Nauk SSSR* **1974**, *229*, 117–123.